Potential Predictability of Two-Year Droughts in the Missouri River Basin

ANDREW HOELL,[a] XIAO-WEI QUAN,[a,b] RACHEL ROBINSON,[a,b] AND MARTIN HOERLING[c]

[a] *NOAA/Physical Sciences Laboratory, Boulder, Colorado*
[b] *Cooperative Institute for Research in Environmental Sciences, University of Colorado Boulder, Boulder, Colorado*
[c] *Department of Civil and Environmental Engineering, University of Colorado Boulder, Boulder, Colorado*

(Manuscript received 27 September 2023, in final form 27 February 2024, accepted 5 March 2024)

ABSTRACT: Potential predictability of 2-yr droughts indicated by low runoff in the consecutive April–September seasons in the upper Missouri River basin (UMRB) and lower Missouri River basin (LMRB) is examined with observed estimates and climate models. The majority of annual runoff is generated in April–September, which is also the main precipitation and evapotranspiration season. Physical features related to low April–September runoff in both UMRB and LMRB include a dry land surface state indicated by low soil moisture, low snowpack indicated by low snow water equivalent, and a wave train across the Pacific–North American region that can be generated internally by the atmosphere or forced by the La Niña phase of El Niño–Southern Oscillation. When present in March, these features increase the risk of low runoff in the following April–September warm seasons. Antecedent low soil moisture significantly increases low runoff risks in each of the following two April–September, as the dry land surfaces decrease runoff efficiency. Initial low snow water equivalent, especially in the Missouri River headwaters of Montana, generates less runoff in the subsequent warm season. La Niña increases the risk of low runoff during the warm seasons by suppressing precipitation via dynamically induced atmospheric circulation anomalies. Model simulations that differ in their radiative forcing suggest that climate change increases the predictability of 2-yr droughts in the Missouri River basin related to La Niña. The relative risk of low runoff in the second April–September following a La Niña event in March is greater in the presence of stronger radiative forcing.

SIGNIFICANCE STATEMENT: Drought spanning consecutive years in the upper Missouri River basin (UMRB) and lower Missouri River basin (LMRB) poses threats to a region whose economy depends on reliable water quantity to support transportation and recreation, adequate water supply for irrigated agriculture, and sufficient streamflow to generate hydroelectric power. We examined physical features in March related to low runoff in the following April–September—low soil moisture, low snow water equivalent, and La Niña events—and examined their effect on the risk of 2-yr drought occurrences. These physical features lead to sustained impacts on the surface water balance. Low snow water equivalent generates less runoff, low soil moisture reduces the runoff efficiency of converting precipitation into runoff, and La Niña inhibits warm-season precipitation and runoff via atmospheric circulation anomalies.

KEYWORDS: La Nina; Teleconnections; Drought; Runoff; Climate prediction; Soil moisture

1. Introduction

Drought in the Missouri River basin (Fig. 1a) threatens the livelihood of a region whose economy depends on riverine transportation, irrigated agriculture, hydroelectric power generation, and aquatic recreation (Mehta et al. 2012; Conant et al. 2018). Droughts spanning consecutive years, as were observed in the 1930s, 1950s, and late 1980s (Fig. 1b; e.g., Ho et al. 2016), especially imperil this region by reducing the buffering capacity that is maintained by the reservoir network along the main stem of the Missouri River and its tributaries (Mehta et al. 2012; U.S. Army Corps of Engineers 2018). The effects of the 1930s "Dust Bowl" were particularly damaging societally (e.g., Hurt 1981) and economically (e.g., Hornbeck 2012) and transcended popular culture based on novels like *The Grapes of Wrath* (Steinbeck 1939). Concerns regarding drought spanning consecutive years have been heightened recently based on reported increases in the frequency of such events in some regions (Wise et al. 2018; Martin et al. 2020) and projected increases in sustained drought throughout the twenty-first century (Wehner et al. 2011; Cook et al. 2015). However, such events have yet to be realized broadly across upper Missouri River basin (UMRB) and lower Missouri River basin (LMRB) regions and have especially not been apparent in streamflow records of the last century. Instead, the observed stream gauge data reveal fewer 2-yr droughts in the recent 3 decades compared to the prior 6 decades in the Missouri River basin (Fig. 1b), associated with upward trends in the region's precipitation (Norton et al. 2014; Hoell et al. 2021, 2023). Nonetheless, 2-yr droughts in the UMRB and LMRB do occur, if irregularly (Fig. 1b), and better understanding of their causes and predictability would inform hydroclimate forecasts and efforts to enhance drought preparedness in this region (National Integrated Drought Information System 2020).

Spatial characteristics, temporal persistence, and physical features related to sustained drought events of the Missouri River basin have been studied, especially those of the 1930s

Supplemental information related to this paper is available at the Journals Online website: https://doi.org/10.1175/JCLI-D-23-0588.s1.

Corresponding author: Andrew Hoell, andrew.hoell@noaa.gov

DOI: 10.1175/JCLI-D-23-0588.1

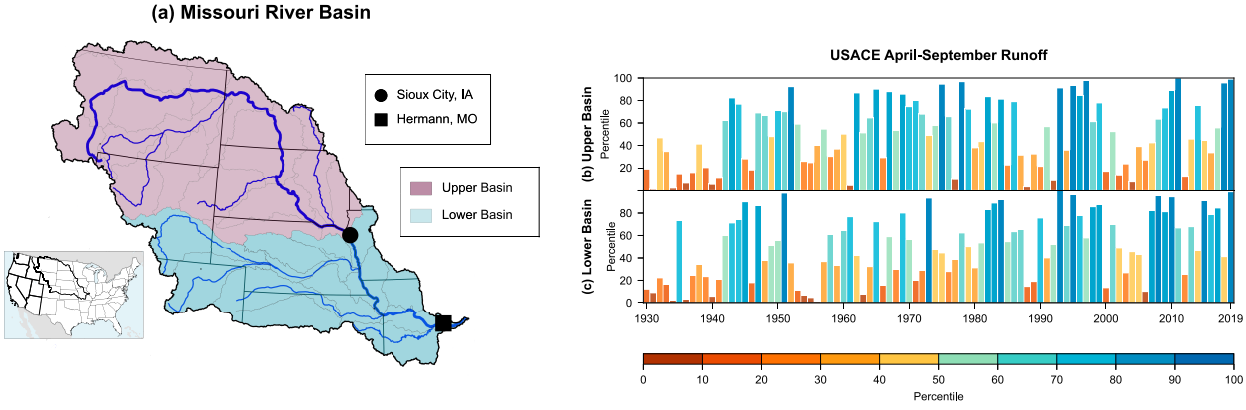

FIG. 1. (a) The Missouri River basin (heavy black polygon). Also indicated are the (UMRB) and LMRB parts of the basin, HUC4 regions used to define the two areas of the basin (thin gray lines), and USACE gauges at Sioux City (circle) and Hermann (square), used to estimate the observed runoff from the UMRB and LMRB, respectively. Based on Hoell et al. (2023) and used with permission from the American Meteorological Society. Time series of April–September runoff percentiles from USACE in the (b) UMRB and (c) LMRB.

and 1950s Dust Bowl era (e.g., Schubert et al. 2004; Hoerling et al. 2009; Cook et al. 2011; Mehta et al. 2012; Heim 2017; Wise et al. 2018; Woodhouse and Wise 2020; McCabe et al. 2023). Flash droughts (e.g., Otkin et al. 2018, 2022; Pendergrass et al. 2020; Christian et al. 2024), characterized by their rapid onset and intensification, have been more common in recent decades (Hoell et al. 2020, 2021, 2023). Given the limited instrumental record (Fig. 1b), sampling hinders our ability to fully understand the characteristics and causes of hydrologic droughts spanning consecutive years.

Physical features related to low runoff in the Missouri River basin have been examined from land surface, atmospheric, and oceanic perspectives. Snowmelt in the UMRB generates approximately one quarter of the entire Missouri River basin runoff measured at Hermann, Missouri (Norton et al. 2014; Qiao et al. 2014; Wise et al. 2018), so it follows that warm-season drought is related to below-average springtime snow water equivalent. Atmospheric circulation patterns related to droughts are often comprised of a persistent wave train of alternating high and low pressure over the Pacific–North American sector with drought-inducing high pressure over the west-central United States (Wise et al. 2018; Hoell et al. 2021), although pattern details differ between events (e.g., Cook et al. 2011; Seager and Hoerling 2014; Burgdorf et al. 2019). The atmospheric wave trains related to drought in the central United States have also been linked to the global patterns of circulation variability describing a circumglobal teleconnection pattern (e.g., Ding and Wang 2005).

These atmospheric circulation patterns may be generated internally by the atmosphere, although they can also be favored by particular states of surface boundary conditions including remote sea surface temperature (SST) variations and local land surface states (e.g., Wu and Kinter 2009; Schubert et al. 2008; Seager and Hoerling 2014; Teng et al. 2019). Examples of droughts in which SSTs forced atmospheric circulations that led to drought in the Missouri River basin include the 1950s (Cook et al. 2011; Hoerling et al. 2009; Seager and Hoerling 2014), whereas the influence of SSTs on the Dust Bowl (Schubert et al. 2004) was comparably weaker (Cook et al. 2011) or perhaps nonexistent (Hoerling et al. 2009). Generalizable SST features related to drought in the Missouri River basin include Pacific and Atlantic SST variability (e.g., McCabe et al. 2004; Wu and Kinter 2009; Wise et al. 2018). The relationship between La Niña and Missouri River basin hydroclimate appears to be inconsistent in the observed record and is further complicated by potential differing relationships between the UMRB and LMRB and between warm and cold seasons (cf. Hoerling et al. 2009; Wu and Kinter 2009; Wise et al. 2018). Links between the Pacific decadal oscillation (PDO; Mantua et al. 1997) and Missouri River basin drought have also been identified (Ting and Wang 1997; McCabe et al. 2004; Mehta et al. 2011), although a more recent study by Newman et al. (2016) has argued that the PDO may be more correlative than causal because it represents the effects of many different processes. Additionally, warm North Atlantic SSTs have been related to Missouri River basin drought (McCabe et al. 2004; Hu et al. 2011; Wise et al. 2018). Linkages between drought in the UMRB and LMRB have been established with land–atmosphere coupling and persistent and/or reemergent soil moisture anomalies (e.g., Wu and Kinter 2009; Mo et al. 2012; Kumar et al. 2019, 2020; Shin et al. 2020; Esit et al. 2021). Regarding land–atmosphere coupling, idealized sensitivity experiments have revealed that low soil moisture in the central United States is related to anomalous atmospheric circulation patterns (Teng et al. 2019). Kumar et al. (2020) found that the land surface coupling increases soil moisture memory during the warm season, but the mechanism by which this occurs remains unknown. Regarding soil moisture memory and soil moisture reemergence, soil moisture has been found to be a better predictor of itself despite limited precipitation predictability (Esit et al. 2021).

In this article, we examine features related to drought in the Missouri River basin with a particular goal to provide a predictive understanding of 2-yr droughts. We address three questions related to drought spanning consecutive years:

TABLE 1. Observed estimates.

Source	USACE	NClimGrid	ERA5	ERSST5
Variables	Streamflow to estimate basin runoff	Temperature Precipitation	Temperature Precipitation Evaporation Runoff Soil moisture 700-hPa wind Snow water equivalent	SSTs
Spatial resolution	Sioux City, Iowa; Hermann, Missouri	0.0417° × 0.0417°	0.25° × 0.25°	2° × 2°
Reference	USACE (2018)	Vose et al. (2014)	Hersbach et al. (2020)	Huang et al. (2017)
Availability	Personal communication, see acknowledgments	https://www.ncei.noaa.gov/data/nclimgrid-monthly/access/	https://www.ecmwf.int/en/forecasts/dataset/ecmwf-reanalysis-v5	https://psl.noaa.gov/data/gridded/data.noaa.ersst.v5.html

- What is the intrinsic persistence of Missouri River basin hydroclimate?
- How do land surface, atmosphere, and ocean features contribute to droughts in warmer and cooler climates?
- Can snow water equivalent, soil moisture, and ENSO state potentially predict 2-yr warm-season droughts?

Concerning hydroclimatic persistence, we document the seasonality and memory of runoff, soil moisture, and precipitation minus evaporation ($P - E$) to establish a baseline from which to examine the predictability of low runoff spanning consecutive years. We use observed estimates and transient climate model simulations during 1940–2019, focusing on the warm season (April–September) because it is the time of year in which the majority of runoff is observed. A transient coupled climate model ensemble based on the Community Earth System Model, version 1 (CESM1; Kay et al. 2015), is used to generate large samples that observed estimates cannot provide. A single transient coupled climate model realization is directly comparable with observed estimates because they indicate a single realization of the climate. Concerning land surface, atmospheric, and oceanic features related to UMRB and LMRB drought, we sample climate model ensembles based on CESM1 during low runoff occurrences to identify the relationships between soil moisture, snow water equivalent, atmospheric circulation, and ENSO. In addition to the CESM1 transient simulations, we use three 1200-yr CESM1 equilibrium simulations in which aspects of the climate system do not vary, which allows us to further isolate the relationships between these aspects of the climate system and Missouri River basin drought. Concerning potential predictability of 2-yr droughts, we quantify the relative risk of low April–September runoff in two consecutive April–September seasons based on soil moisture, snow water equivalent, and ENSO in March prior to the first warm season.

This article is organized as follows. In section 2, we present the data and methods used. In sections 3 and 4, we present the results concerning physical features and potential predictability of drought spanning consecutive years in the UMRB and LMRB. In section 5, we summarize principal conclusions based on the three questions posed previously.

2. Data and methods

a. *Observed estimates and model simulations*

We use observed estimates during 1920–2019 to document hydroclimatic variability and drought in the UMRB and LMRB and their relationships with land surface states, atmospheric circulation, and SSTs (Table 1). The U.S. Army Corps of Engineers (USACE) naturalized Missouri River flow at Sioux City, Iowa, and Hermann, Missouri, are used to estimate runoff originating from the UMRB and LRMB, respectively (Fig. 1a). This naturalized flow estimate, also used in Hoell et al. (2023), removes the effects of dams, diversions, and withdrawals, which allows for it to be compared to historical hydroclimatic variability in each subbasin of the Missouri River catchment. We use gridded estimates from the fifth major global reanalysis produced by ECMWF (ERA5) and the NOAA U.S. Climate Gridded Dataset (NClimGrid), the former a reanalysis based on the model assimilation of observed conditions and the latter based on interpolating historical station observations to a grid. Estimates of SSTs are from the Extended Reconstructed SST, version 5 (ERSST.v5; Huang et al. 2017), and estimates of atmospheric circulation and land surface states are from ERA5.

We use simulated conditions from CESM1 integrated on a 0.9° × 1.25° latitude–longitude horizontal grid to contextualize hydroclimatic variability and to diagnose predictability sources for 2-yr droughts in the UMRB and LMRB. Four climate model experiments are used (Table 2): one consists of 40 fully coupled transient realizations during 1920–2019 in which natural and anthropogenic radiative forcing vary in time (CESM1-Transient) and the remaining three consist of 1200-yr equilibrium simulations in which the radiative forcing remains the same. All components of the climate system in two of the equilibrium experiments are simulated, with one driven by radiative forcing from 1850 (B1850) and the other by radiative forcing from 2000 (B2000). A third equilibrium experiment is driven by radiative forcing from 1850, but ocean conditions are set to a repeating annual cycle of average conditions from the B1850 simulation (F1850). Like our observed analyses, we diagnose temperature, precipitation, evaporation, runoff, soil moisture, snow water equivalent, 700-hPa wind, and SSTs.

TABLE 2. Climate model simulations.

Climate model	CESM1	CESM1	CESM1	CESM1
Experiment	CESM1-Transient	B2000	B1850	F1850
Simulation type	Transient	Equilibrium	Equilibrium	Equilibrium
Realizations	40	—	—	—
Duration	1940–2021	1200 years	1200 years	1200 years
Radiative forcing	Historical before 2005 (Taylor et al. 2012) RCP8.5 after 2005 (Taylor et al. 2012)	Year 2000	Year 1850	Year 1850
SST forcing	Simulated	Simulated	Simulated	Prescribed
Source	https://www.cesm.ucar.edu/projects/community-projects/LENS/data-sets.html	See data availability statement	https://www.cesm.ucar.edu/community-projects/lens/instructions#ESG	https://www.cesm.ucar.edu/community-projects/lens/instructions#ESG

b. *Missouri River basin*

We separate the entire drainage area into UMRB and LMRB subbasins (Fig. 1a). Following an approach that is consistent with common research and operational definitions of the Missouri River basin (Livneh et al. 2016; U.S. Army Corps of Engineers 2018; Badger et al. 2018; Hoell et al. 2023), the UMRB and LMRB are defined by river routing across second-level Hydrologic Unit Code (HUC4; Fig. 1a, gray polygons) in the first-level Hydrologic Unit Code (HUC2; Fig. 1a, black polygon) that defines the Missouri River basin (Hoell et al. 2023). UMRB runoff flows to the main stem of the Missouri River above Sioux City, Iowa (Fig. 1a, dot), and LMRB runoff flows to the main stem of the Missouri River above Hermann, MO (Fig. 1a, square). Estimates of conditions in the UMRB and LMRB based on gridded data are computed from averages of all points in the areas that define each subbasin.

Additional reasons for separating the Missouri River basin into the UMRB and LMRB include the reports of changes in the relationship between the two regions during drought (Woodhouse and Wise 2020) and an April–September runoff correlation between the two basins of 0.41 (Fig. 1b). As noted by Hoell et al. (2023), this perspective differs from some other studies of the hydrologic catchment, many of which have focused on smaller areas of the Missouri River basin like the headwaters (Wise et al. 2018; Martin et al. 2020; Woodhouse and Wise 2020; Frederick and Woodhouse 2020), the Milk River (Martin and Pederson 2022), and the southeastern part of the catchment (Norton et al. 2014; Wise et al. 2018; Woodhouse and Wise 2020).

c. *Drought and potential predictability*

Our examination of UMRB and LMRB drought focuses on attendant and antecedent land surface, atmospheric, and oceanic features associated with low warm-season runoff. Warm-season drought is defined as April–September seasons in which UMRB and LMRB runoff falls below the 20th percentile. This definition is consistent with drought categories from the U.S. Drought Monitor (Svoboda et al. 2002). Atmospheric and oceanic features related to low UMRB and LMRB warm-season runoff are identified based on the composite analysis of attendant 700-hPa wind and SST anomalies, respectively. Antecedent land surface features related to low UMRB and LMRB warm-season runoff are identified based on composite analysis of standardized 1-m soil moisture and snow water equivalent standardized anomalies during the prior March. Percentiles, standardized anomalies, and anomalies in observed estimates and CESM1-Transient are computed based on 1940–2019, the common period of record of the data. For the equilibrium simulations, percentiles, standardized anomalies, and anomalies are computed based on the entire 1200-yr record relative to their own climate to highlight drought variability.

The four CESM1 climate model experiments are used in different ways to diagnose UMRB and LMRB drought and its potential predictability. Individual CESM1-Transient realizations are compared to observations because both indicate a single realization of the climate in which radiative forcing varies. This comparison is used to identify physical features related to UMRB and LMRB drought and assess the model's ability to simulate these features. The equilibrium climate model experiments are used to isolate the effect of certain aspects of the earth system on UMRB and LMRB drought. SSTs do not vary from the annual cycle in the F1850 simulation, and we use them to determine the effect of atmosphere and land surface processes on drought. The B1850 and B2000 simulations differ in their radiative atmospheric forcing, and we use these simulations to judge how the radiative forcing is related to drought variability, as well as atmosphere, land surface, and ocean behaviors, which all vary freely in each simulation.

We diagnose the potential predictability of low UMRB and LMRB runoff in two consecutive April–September based on ENSO, 1-m soil moisture, and snow water equivalent states in March prior to the first warm season. Our metric for diagnosing potential predictability is the relative risk ratio. We use the relative risk ratio to compare the frequency of April–September runoff falling below the 20th percentile when ENSO and land surface conditions are met in March to the frequency of April–September runoff falling below the 20th percentile when those conditions are not met in March in the equilibrium climate model simulations. A relative risk of greater than 1 indicates that conditions are related to an increased occurrence of low runoff while a relative risk of less

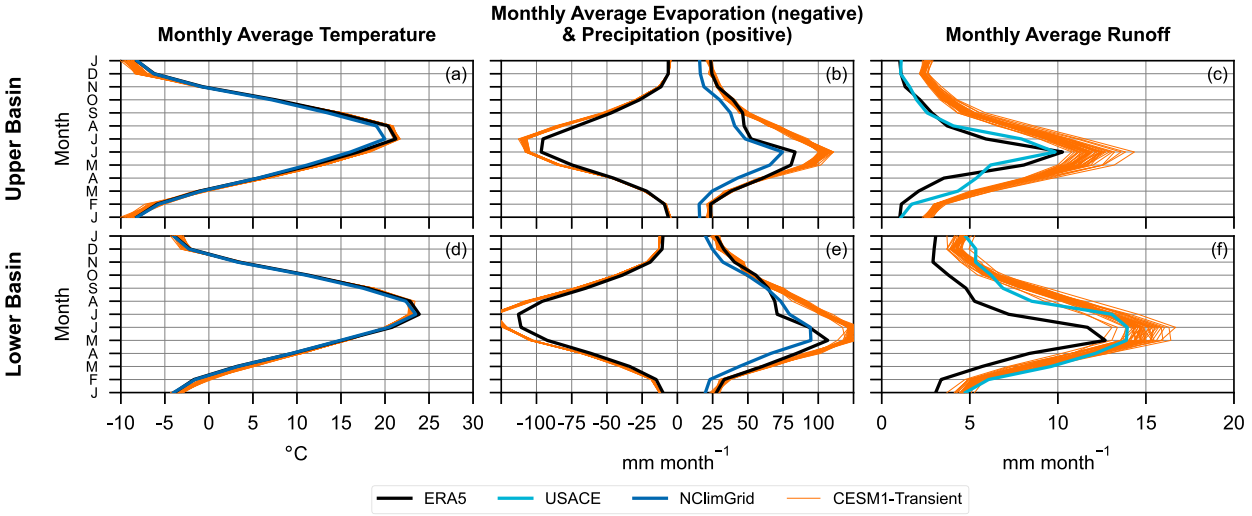

FIG. 2. For 1940–2019 in the (top) UMRB and (bottom) LMRB, monthly average (left) temperature (°C), (center) evaporation (mm month^{-1}; negative values) and precipitation (mm month^{-1}; positive values), and (right) runoff (mm month^{-1}). ERA5 is indicated by the black lines, NClimGrid is indicated by the blue lines, CESM1-Transient realizations are indicated by the thin orange lines, and USACE runoff is indicated by the cyan lines.

than 1 indicates that conditions are related to a decreased occurrence of low runoff. The conditions we focus on are La Niña, El Niño, low 1-m soil moisture, high 1-m soil moisture, low snow water equivalent, and high snow water equivalent. La Niña and El Niño are defined based on threshold exceedances of SSTs averaged in the Niño-3.4 region (5°S–5°N and 120°–170°W). Thresholds of −0.5 and 0.5 standardized departures of the Niño-3.4 index are used to define La Niña and El Niño, respectively. 20th and 80th percentile thresholds of 1-m soil moisture and snow water equivalent states are used to identify wet and dry conditions, respectively.

We construct confidence intervals based on the bootstrapping approach described by Efron (1979). Confidence intervals are estimated by repeatedly (10 000 times) performing a calculation based on random draws with replacement from a population. The 95% confidence interval (2.5th percentile and 97.5th percentile) is used because there is less than a 5% chance of the values at these percentiles occurring randomly ($p < 0.05$). Concerning relative risk, statistically significant relative risks are found when the 95% confidence interval exceeds or falls below 1.

3. Hydroclimatic persistence

We begin by examining the seasonality and persistence of hydroclimatic quantities in observed estimates and transient climate model simulations during 1940–2019. Monthly average conditions in observations reveal a distinct seasonal cycle in the region's hydroclimate, with temperatures, precipitation, evaporation, and runoff all reaching their maxima during April–September and minima during October–March (Fig. 2). Regarding temperatures, monthly average temperatures based on ERA5 and NClimGrid reveal the highest (lowest) observed monthly temperatures in July–August (December–February) in both subbasins (Fig. 2, left column). Monthly average temperatures from the CESM1-Transient simulations closely match these observations counterparts, with little spread across the 40 realizations, which demonstrates the strong constraint of the seasonal cycle.

Precipitation and evaporation also display distinct seasonal cycles in the UMRB and LMRB, reaching maxima during late spring and summer and minima during the cold season (Fig. 2, center column). NClimGrid and ERA5 precipitation in both UMRB and LMRB reach their maxima in May and June, with appreciable precipitation in the lead—up to these months, through summer, and into autumn. ERA5 evaporation closely follows the seasonal cycles of temperature and precipitation, given the effect of temperatures on evaporative demand by the atmosphere and precipitation on water availability. CESM1-Transient monthly averages follow the NClimGrid and ERA5 seasonal cycles but reveal a positive bias in precipitation and evaporation, neither of which can be reconciled with sampling variability.

Given temperature, precipitation, and the resulting hydrological balance of the land surface, observed runoff also exhibits a distinct seasonal cycle in the UMRB and LMRB, reaching maxima in late spring and early summer and minima in the cold season (Fig. 2, right column). While the ERA5 and USACE seasonal cycles align, it is important to note that there is observational uncertainty across these estimates. Both differ in their magnitudes, particularly in the LMRB where ERA5 simulates less runoff compared to USACE naturalized flow. The 40 CESM1-Transient realizations simulate a seasonal runoff cycle that closely resembles that of ERA5 and USACE, although once again a high bias in runoff compared to observed estimates is evident likely due to the high precipitation bias in the model during the warm season. Prior to using these data to diagnose drought in the Missouri River basin, it is important to note that potential biases could affect the results and interpretation.

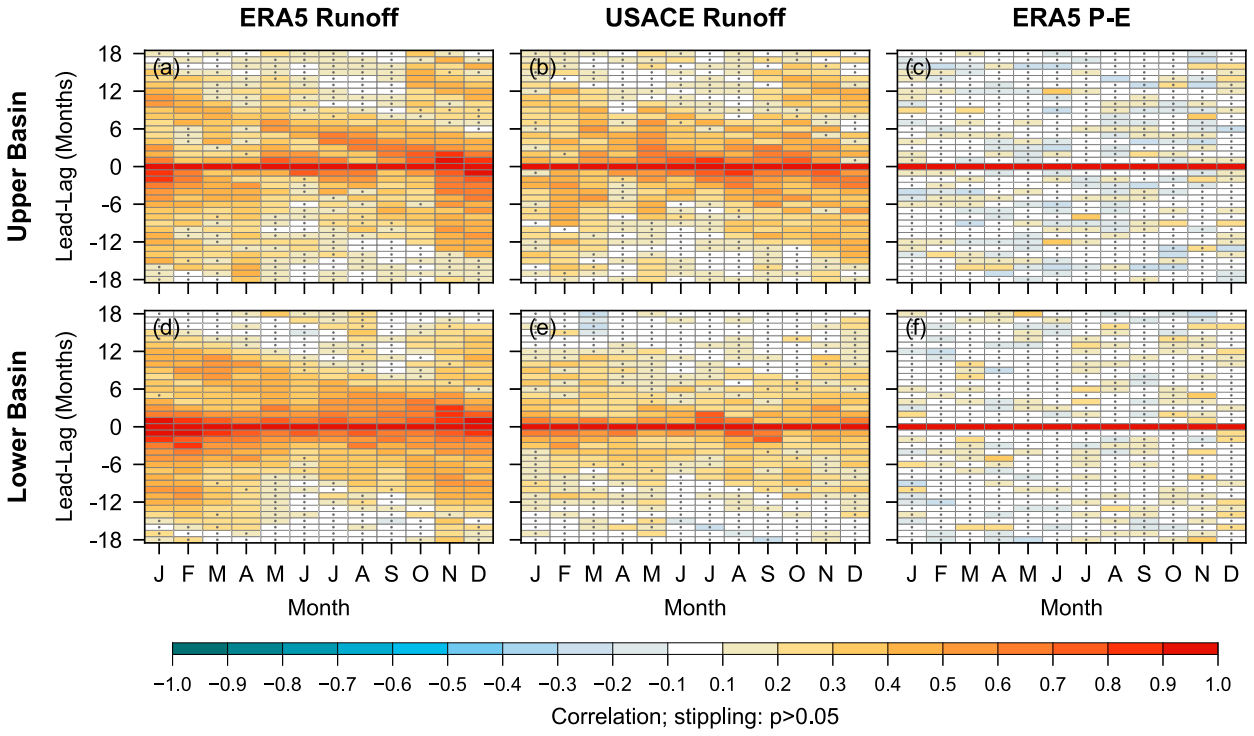

FIG. 3. For 1940–2019 in the (top) UMRB and (bottom) LMRB, monthly lead–lag correlations of (left) ERA5 runoff, (center) USACE runoff, and (right) ERA5 $P - E$. Positive values on the ordinate indicate the correlation between a given month on the abscissa and a future month. Negative values on the ordinate indicate the opposite. Stippling indicates the correlations that are not statistically significant at $p < 0.05$.

Lead–lag correlations of runoff and $P - E$ centered on each month in ERA5 and USACE observed estimates (Fig. 3) are used to diagnose hydroclimatic persistence in the UMRB and LMRB. In both subbasins, we find systematic month-over-month persistence in runoff, but no persistence in $P - E$. There is, therefore, inherent memory in the land surface that acts to constrain surface runoff. The seasonality and magnitude of the serial runoff correlations based on ERA5 (Fig. 3, left column) and USACE (Fig. 3, right column) indicate runoff persistence between the warm season, the following cool season, and the beginning of the next warm season, indicating that land surface memory plays a role in shaping runoff during the following 6–12 months. Although both ERA5 and USACE indicate the systematic persistence of runoff based on statistically significant serial runoff correlations from each month, the magnitude of these correlations between both observed analyses differs at given leads and lags as a function of season. $P - E$ based on ERA5 at all leads and lags centered on each month are not systematically correlated with one another in the UMRB and LMRB, indicating no persistence in the simultaneous supply and demand of moisture by the atmosphere (Fig. 3, right column).

To further explore hydroclimatic persistence in the UMRB and LMRB, Fig. 4 presents lead–lag runoff and $P - E$ correlations centered on March. The observed estimates are compared to those based on the 40 CESM1-Transient realizations. March is presented because it immediately precedes the seasonal wet season for much of the Missouri River basin so we can quantify how initial conditions in that critical month constrain hydroclimate during the following April–September. Statistically significant serial correlations in runoff for up to 9 months are found for both the UMRB and LMRB, with positive correlations up to 18-month leads, which indicate runoff memory from before the first prior April–September warm season into the next warm season (Fig. 4, left column). Although differences in ERA5 and USACE serial correlations demonstrate observational uncertainty owing to the differences in their runoff computations, both estimates indicate statistically significant serial correlations spanning the prior April–September warm season into the next warm season, with the former generally indicating stronger serial correlation.

The lead–lag correlations for the two observed estimates generally fall within the spread of the 40 CESM1 realizations for the UMRB and LMRB, indicating that CESM1 simulates reasonably realistic runoff memory. Note also the appreciable spread in the serial runoff correlations among the CESM1-Transient realizations, which demonstrates a sampling range for these serial correlations even within 80-yr climate records. One can, thus, not reject the hypothesis that the model runoff persistence statistics are inconsistent with observations. One notable exception concerns the model's minimum in serial persistence in the UMRB for the prior February (the blue lines in Fig. 4a), which may be due to a model bias in simulating frozen ground, and/or the amount and type of wintertime

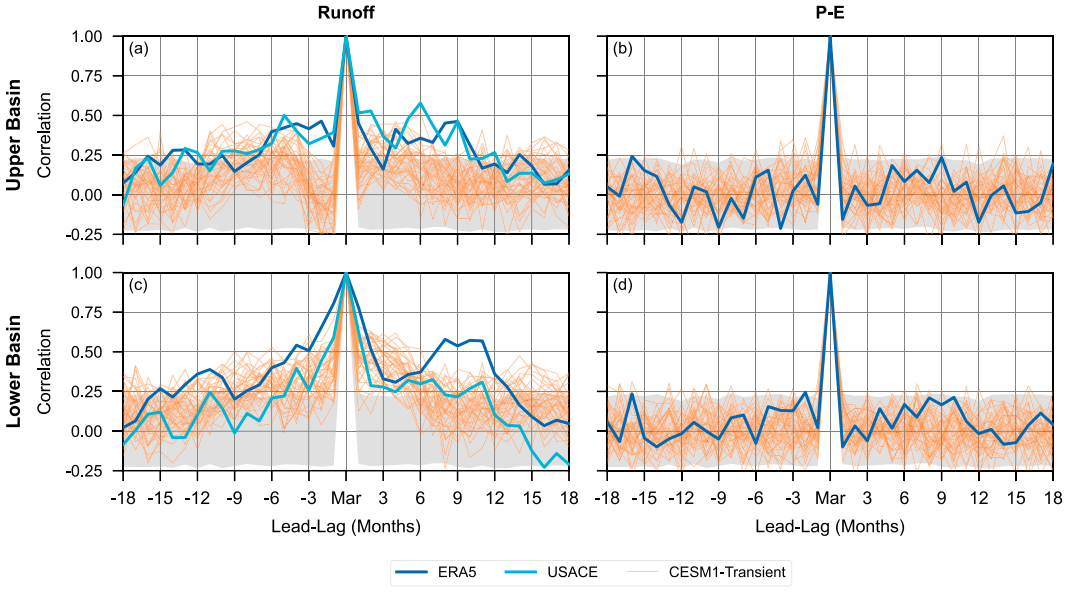

FIG. 4. For 1940–2019 in the (top) UMRB and (bottom) LMRB, monthly lead–lag correlations from March for (left) runoff and (right) $P - E$. Blue lines indicate the ERA5, orange lines indicate the CESM1-Transient realizations, and the cyan lines indicate the USACE runoff. Positive values on the ordinate indicate the correlations between March and a future month. Negative values on the ordinate indicate the opposite. The gray shading indicates the 95% confidence interval.

precipitation (Fig. 2). The contrast in memory of the land surface runoff versus $P - E$ is again striking. Consistent with Fig. 3, there is no systematic persistence in UMRB and LMRB $P - E$ from March in observed estimates nor in the CESM1-Transient realizations. This result reinforces that there is no memory in the simultaneous supply and demand of moisture by the atmosphere (Fig. 4, right column).

It is, therefore, evident that runoff persistence arises from properties of the land surface, not the atmosphere. To demonstrate this further, Fig. 5 presents lead–lag correlations of ERA5 soil moisture estimates centered on March in the context of the CESM1-Transient realizations (Fig. 5). Two soil depths are considered, 1–30 cm and the other to 1 m, to determine how layer depth determines land surface memory. Serial soil moisture correlations from March indicate statistically significant persistence for the 30-cm and 1-m layers in the UMRB and LMRB (cf. Fig. 5, left and right columns), although correlations are generally larger in the latter layer, given that it is less exposed to surface processes. Soil moisture is most persistent in the cold season leading up to spring, particularly in the UMRB, since this is the time of year when less precipitation is observed and the ground is frozen (Fig. 2). Conversely, soil moisture is less persistent in springtime at the beginning of the wet season that immediately follows March since this is a time of year in which $P - E$ exceeds 0 on average (Fig. 2, center column). Statistically significant serial soil moisture correlations are not found greater than 1 year following March in either subbasin (Fig. 5), which suggests that relationships between soil moisture and future land surface states—including runoff—are not found when all initial land surface states in an 80-yr period are considered. However, we will later show that low soil moisture in March is related to low runoff in the two following April–September, which suggests the importance of extreme land surface states to runoff predictability.

4. Drought and its potential predictability

a. *Transient climate*

We turn our attention to drought in the UMRB and LMRB to identify physical features that could potentially predict low runoff spanning two consecutive April–September. Based on ERA5 observed estimates and CESM1-Transient realizations, low April–September runoff in the UMRB and LMRB are related to concurrent atmospheric conditions that include anticyclonic circulation over the north-central United States (vectors in Fig. 6) and oceanic features that include La Niña (shading in Fig. 6). The concurrent SST relation, although significant in the model ensemble based on the average of 40 realizations, is absent in the observed estimates. Here, it is important to note that a single realization of climate provided by the observed history is akin to a single CESM1 realization over the same period. The results in the supplementary material (see Figs. S1 and S2 in the online supplemental material) illustrate the considerable sampling variability in the SST relationships to Missouri River basin drought among such realizations. The inherent sampling noise evident even in the concurrent ERA5 wind composites indicates a noisy perspective, although common features related to drought include anticyclonic circulation over the Northern Rockies associated with UMRB drought and anticyclonic circulation over the central United States associated with LMRB drought (Fig. 6, left column). The analogous concurrent wind

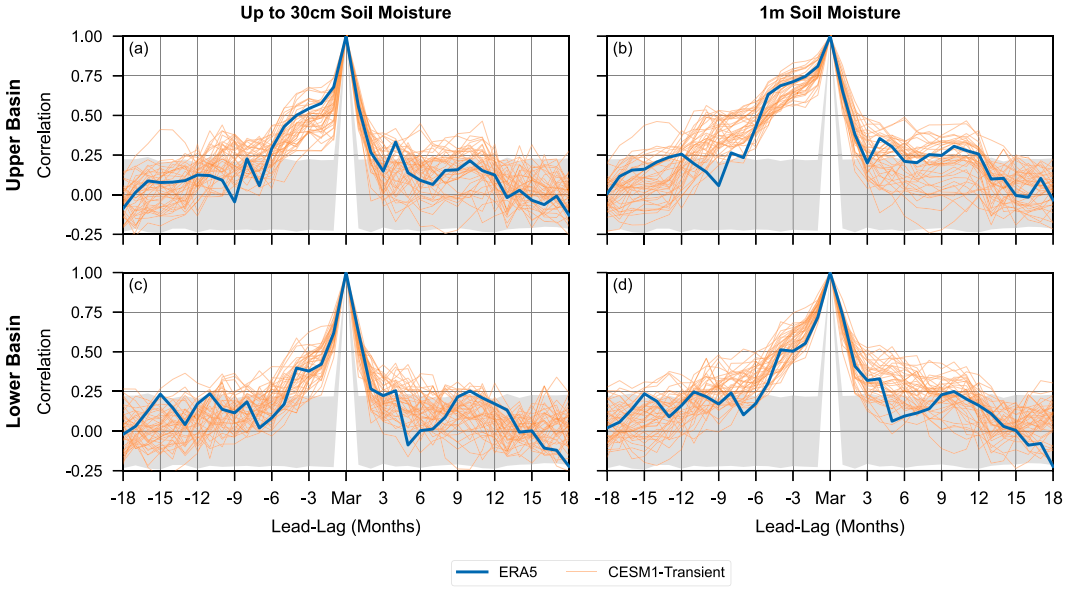

FIG. 5. For 1940–2019 in the (top) UMRB and (bottom) LMRB, monthly lead–lag correlations from March for (left) up to 30-cm soil moisture and (right) 1-m soil moisture. Blue lines indicate ERA5 and orange lines indicate CESM1-Transient realizations. Different layer depths in the left column for ERA5 (28 cm) and CESM1-Transient (21 cm) are considered because data are not available at the same layer depths. Positive values on the ordinate indicate the correlations between March and a future month. Negative values on the ordinate indicate the opposite. The gray shading indicates the 95% confidence interval.

composites for each of the 80-yr CESM1-Transient realizations shown in Figs. S1 and S2 indicate similarly noisy features. The most prominent feature across the CESM1 realizations is the presence of anomalous anticyclonic circulation over the central United States related to UMRB and LMRB drought similar to that of the ERA5 observed estimates, which indicates the importance of the atmospheric circulation. A concurrent SST anomaly pattern resembling La Niña appears to be a preferred ocean state in the CESM1 ensemble, a feature appearing in many, though not all, of the CESM1-Transient realizations (Figs. S1 and S2). A variety of SST anomaly patterns related to UMRB and LMRB drought in April–September, however, suggest that SSTs may not be a requirement nor offer a strong constraint on drought likelihoods in the Missouri River basin, a topic we will further explore below.

The SST and 700-hPa wind anomaly composite related to low runoff in all 40 CESM1-Transient realizations clarifies conditions associated with UMRB and LMRB drought in April–September, given the large sample provided by the ensemble simulations (Fig. 5, right column). This analysis reveals distinct atmospheric and oceanic features related to Missouri basin drought. From the atmospheric perspective, concurrent anticyclonic circulation over the central United States is a prominent feature, which centered just to the west of the Missouri River basin is accompanied by anomalous precipitation-reducing subsidence (not shown) and opposes the flow of moisture into the region, thereby resulting in low runoff. A second anticyclone is present over the North Pacific Ocean, which, while not directly forcing Missouri River basin drought, may be part of the same wave train as the anticyclonic circulation over North America associated with La Niña, which is prominent in the SST anomaly composite. Regarding concurrent relationships with La Niña, low runoff in both the UMRB and LMRB is associated with statistically significant below-average SSTs in the tropical east-central Pacific Ocean, above-average SSTs in the tropical west Pacific. Above-average SSTs in the North Pacific are also prominent in the CESM1 SST anomaly composite in the same area as anomalous anticyclonic atmospheric circulation, which would further aid in the maintenance of the warm SSTs (e.g., Alexander et al. 2002).

Focusing now on land surface preconditioning of low runoff in a transient climate, we find that low 1-m soil moisture in March is related to low runoff in the following April–September in the UMRB and LMRB based on ERA5 and the CESM1-Transient realizations (continental shading in Fig. 6). The same perspective for each of the 40 CESM1-Transient realizations is provided in Figs. S1 and S2 in the UMRB and LMRB, respectively. The pattern of 1-m March soil moisture related to low warm-season runoff for an 80-yr trace of the climate based on ERA5 (Fig. 6, left column) and CESM1 realizations (Figs. S1 and S2) are noisy due to sampling, yet reveal common features that include low antecedent soil moisture in the Missouri basin itself. The same composite conditions, but including all samples from the 40 CESM1-Transient realizations (Fig. 6, right column), clarify 1-m soil moisture in March related to low runoff in the following April–September, given the many droughts considered. This analysis reveals a close relationship between low warm-season runoff and antecedent soil moisture in the UMRB and LMRB in addition to milder, yet statistically significant relationships elsewhere in the United States. In the UMRB, the March 1-m soil moisture pattern related to low April–September

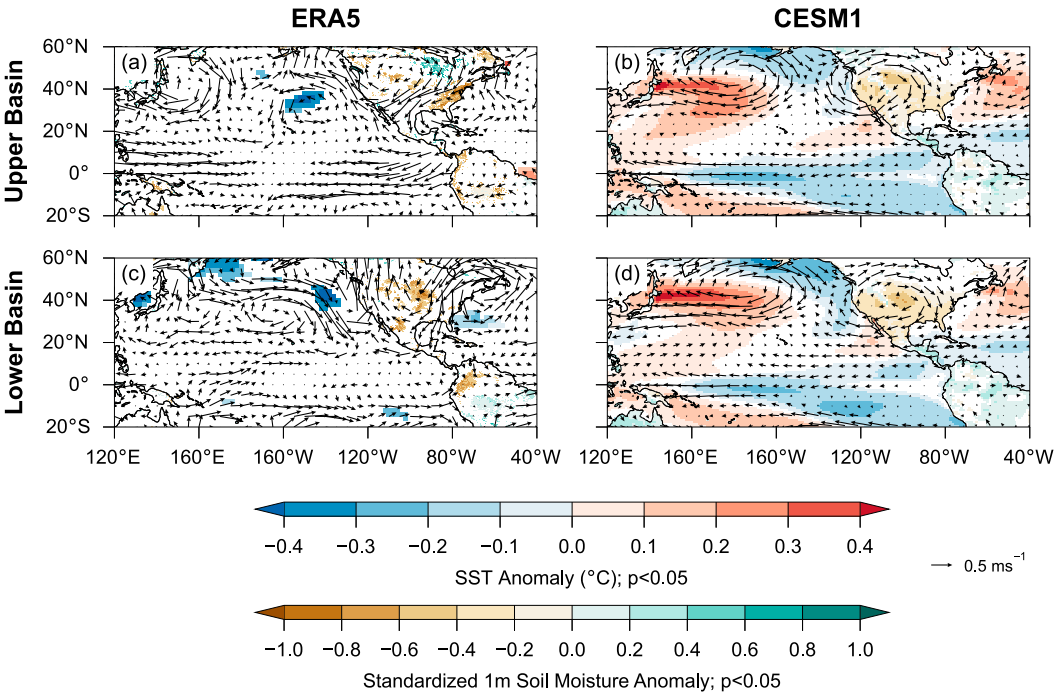

FIG. 6. When April–September basin average runoff is in the lower 20th percentile during 1940–2019, composite concurrent 700-hPa wind (vectors; m s^{-1}) and SST anomalies (blue-red shading; °C) and composite antecedent standardized 1-m soil moisture anomaly (brown-green shading; standard deviations) during the prior March for the (left) ERA5 and (right) 40 CESM1-Transient realizations in the (top) UMRB and (bottom) LMRB. Shading for SSTs and 1-m soil moisture indicates anomalies that are statistically significant at $p < 0.05$. Conditions for the UMRB and LMRB in each of the 40 CESM1 transient realizations are shown in Figs. S1 and S2, respectively.

runoff indicates the strongest relationships in the Southwest and Southeast United States (Fig. 6b). In the LMRB, this perspective indicates the strongest relationships resembling a precipitation pattern related to La Niña, with large anomalies in the southern tier of the United States, which suggests a role for La Niña on the persistence of hydrological drought into the following year's warm season (Fig. 6d).

We also find that low snow water equivalent in March in the Missouri River basin is related to low runoff in the following April–September in the UMRB and LMRB based on ERA5 and CESM1-Transient realizations (Fig. 7). The same perspective for each CESM1-Transient realization is provided in Figs. S3 and S4in the UMRB and LMRB, respectively. The pattern of snow water equivalent anomalies in individual traces of the climate like ERA5 (Fig. 7, left column) and CESM1-Transient (Figs. S3 and S4) indicates the differences between each realization, but all share generalizable features with conditions compiled over all CESM1-Transient realizations (Fig. 7, right column). That is, drought is related to low snow water equivalent in the colder and elevated areas of the Missouri River basin that generate considerable runoff like the headwaters region in Montana (see Norton et al. 2014; Qiao et al. 2014; Wise et al. 2018). This is especially true for the UMRB (Fig. 7, top row), where snow-generated runoff from the upper reaches of the basin is considerable. By contrast, the precipitation seasonal cycle and the lower elevations of the LMRB result in less contribution to runoff by snowmelt, which, in turn, leads to a weaker relationship between April–September runoff and antecedent snowpack.

b. *Equilibrium climate simulations*

We use equilibrium simulations F1850, B1850, and B2000 to disentangle relationships between land–ocean–atmosphere features and low April–September runoff in the UMRB and LMRB (Fig. 8). The F1850 simulation, in which ocean conditions are prescribed to a repeating annual cycle, indicates that the atmosphere alone can lead to drought in the Missouri River basin via anomalous circulations confined to the Pacific–North American sector. A prominent anticyclone over the central United States is related to UMRB and LMRB drought in April–September, as indicated by 700-hPa wind anomalies related to low runoff (Fig. 8, left column). The anticyclones related to UMRB and LMRB drought over the central United States are similar in location and position to those identified in the CESM1-Transient realizations (cf. Fig. 8, left column, to Fig. 6, right column). Such similarity indicates that the drought in the transient realizations can be caused by processes internal to the atmosphere only. UMRB and LMRB drought in the F1850 simulation is also related to two additional atmospheric circulation centers in the North Pacific—cyclonic circulation to the west of North America and anticyclonic circulation to the southwest of the Aleutian Islands—which is indicative of the relationship between the Missouri River basin

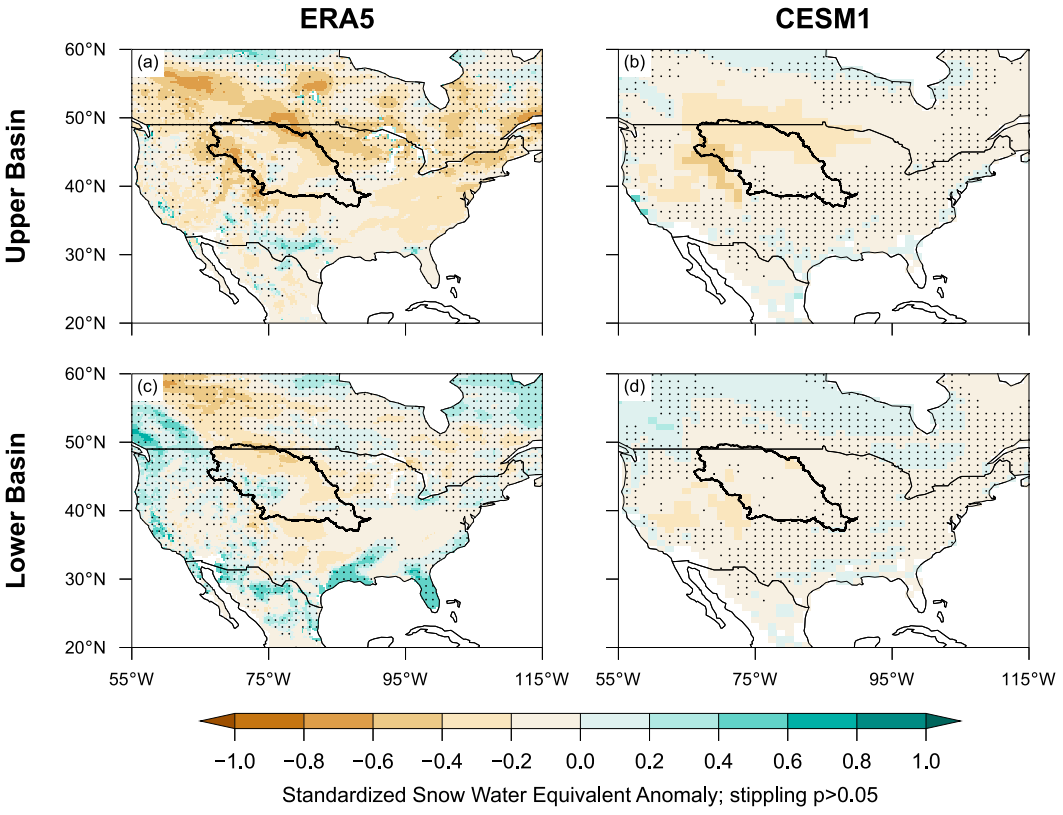

FIG. 7. Composite March standardized snow water equivalent anomaly when basin runoff during the following April–September is in the lower 20th percentile during 1940–2019 for the (left) ERA5 and (right) 40 CESM1 transient realizations in the (top) UMRB and (bottom) LMRB. Stippling indicates the standardized departures that are not statistically significant at $p < 0.05$. Conditions for the UMRB and LMRB in each of the 40 CESM1-Transient realizations are shown in Figs. S3 and S4, respectively.

drought and an atmospherically generated wave train spanning the Pacific–North American sector.

The inclusion of coupled SST variability in the B1850 and B2000 simulations affirms that the atmospheric circulation roots for Missouri River basin drought (Fig. 8, center and right columns). However, there are notable differences between this wave train and that identified in the atmosphere-only (F1850) simulation. Specifically, the circulation centers that comprise the wave train in a climate without SST variability are weaker than in a climate with SST variability, which indicates a role for SSTs in modulating the magnitude and nature of the atmospheric circulation related to Missouri River basin drought. Additionally, the scale of the circulation in the coupled models is larger, with connections to the tropics evident that are indicative of La Niña influences. The contributions of tropical SST forcing to the circulation pattern also yield a North Pacific SST signature in the coupled models that is consistent with the well-known atmospheric bridge mechanism linking tropics and extratropics (e.g., Alexander et al. 2002). It cannot be discounted, however, that inherent extratropical SST variations alone could contribute to a drought-producing extratropical wave train over the Pacific–North American sector.

The B1850 and B2000 equilibrium simulations show that both intrinsic atmosphere and ocean variations can either individually or collectively lead to drought in the Missouri River basin. The similarity with results from the CESM1-Transient realizations indicates that increasing radiative forcing during 1940–2019 is not a necessary factor for MRB drought. However, it is intriguing to note that the relationship between La Niña and MRB drought during April–September is stronger in a climate with enhanced radiative forcing (cf. Fig. 8, center and right columns). Anomalous SSTs related to low April–September runoff in both the B2000 and B1850 are similar in sign and pattern, but the composite tropical Pacific SST anomalies in the B2000 simulation related to Missouri River basin drought are a factor of two larger than its B1850 counterparts. Moreover, the sign and patterns of anomalous 700-hPa winds across the Pacific–North American sector related to low April–September are similar in the B2000 and B1850 simulations, though likewise differ in the magnitude of the wind anomalies, with the former stronger than the latter. This also suggests that stronger greenhouse gas forcing leads to stronger atmospheric circulation anomalies in tandem with La Niña when related to UMRB and LMRB drought.

We further identify the relationship between La Niña and Missouri River basin drought in Fig. 9 by showing composite SSTs and atmospheric circulation when both low UMRB and LMRB runoff and cold equatorial central and eastern Pacific

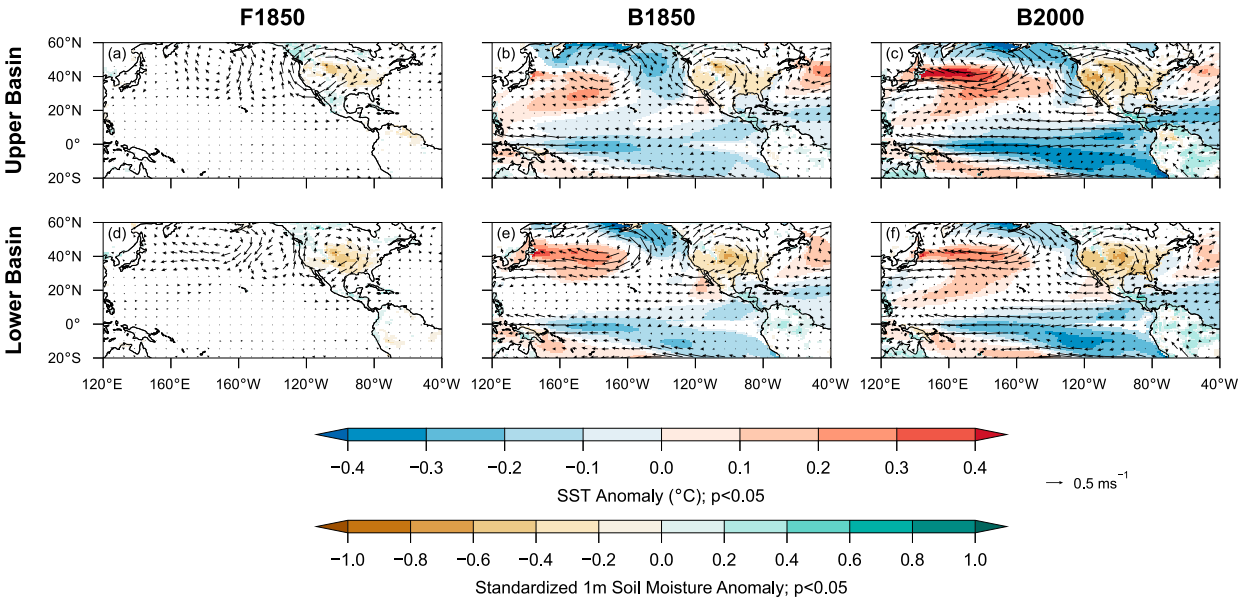

FIG. 8. When April–September basin average runoff is in the lower 20th percentile during 1940–2019, composite concurrent 700-hPa wind (vectors; m s^{-1}) and SST anomalies (blue–red shading; °C) and composite antecedent standardized 1-m soil moisture anomaly (brown–green shading; standard deviations) during the prior March for the (left) F1850, (center) B1850, and (right) B2000 equilibrium simulations in the (top) UMRB and (bottom) LMRB. Shading for SSTs and 1-m soil moisture indicates anomalies that are statistically significant at $p < 0.05$. Note that there is no SST variability from mean conditions in the F1850 simulation as SSTs are prescribed to a repeating annual cycle from the B1850 simulation.

states are met in the B1850 and B2000 simulations. This perspective more clearly identifies the relationship between drought and La Niña than Fig. 8 because it omits cases in which La Niña is not operating. A stronger relationship between UMRB and LMRB drought and Pacific SSTs is found in both simulations in Fig. 9 compared to Fig. 8 as well as a wave train of alternating high and low pressure areas emanating from the tropics, to the North Pacific Ocean, and across North America in both equilibrium simulations. Moreover, SST and circulation anomalies are stronger in the B2000 simulation in which radiative forcing is stronger than the B1850 simulation.

Also using equilibrium simulations F1850, B1850, and B2000 shown in Fig. 8, we examine the relationships between 1-m soil moisture in March and low runoff during the following April–September in the presence of forcing only by the atmosphere and forcing by both the atmosphere and oceans. The F1850 simulation reveals that in the presence of only atmospheric variability that 1-m March soil moisture is significantly related to drought in the next warm season in an area local to, and just to the east of, the Missouri River basin (Fig. 8, left column). The localized nature of these relationships contrasts those same relationships in the B1850 and B2000 simulations, which are widespread across North America (Fig. 8, center and right columns). These widespread relationships between 1-m March soil moisture and low runoff in the following April–September suggest that the addition of oceanic forcing leads to a widespread dry land surface state that includes the Missouri River basin. Moreover, the magnitude of the 1-m soil moisture standardized anomalies related to warm-season low runoff in the UMRB and LMRB is larger and more widespread in the B2000 simulation compared to the B1850 simulation. The more intense and widespread low soil moisture in the B2000 simulation suggests an important role of a warmer climate in leading to such occurrences in the Missouri River basin. These conditions are consistent with stronger La Niña events described previously, which lead to stronger atmospheric anomalies that increase the magnitude and footprint of low 1-m soil moisture that precedes low runoff occurrences in the Missouri River basin.

Further examination of 1-m soil moisture in March and runoff in the following April–September suggests that a mechanism responsible for low warm-season runoff to follow a dry land surface state concerns runoff efficiency (the fraction of precipitation that becomes runoff). This is based on Fig. 10, which relates UMRB and LMRB 1-m soil moisture in March to runoff in the following April–September, and its runoff efficiency in equilibrium simulations F1850, B1850, and B2000. All equilibrium simulations indicate that low antecedent soil moisture is associated with lower warm-season runoff efficiency and, hence, runoff. That is, when the land surface state before April–September is dry, less runoff is generated by the same amount of precipitation because more precipitation is used to moisten the land surface. The runoff efficiency differs by a factor of 2 between initial dry versus wet soil moisture states. Note that the constraint of soil moisture on subsequent runoff is not via a change in the subsequent rainfall during the warm season (that signal is found to be negligible in the model), but rather via a dramatic change in the fractional conversion of the summer rains into runoff. It is also important to note that these relationships are similar across the equilibrium simulations regardless of SST variability and radiative forcing,

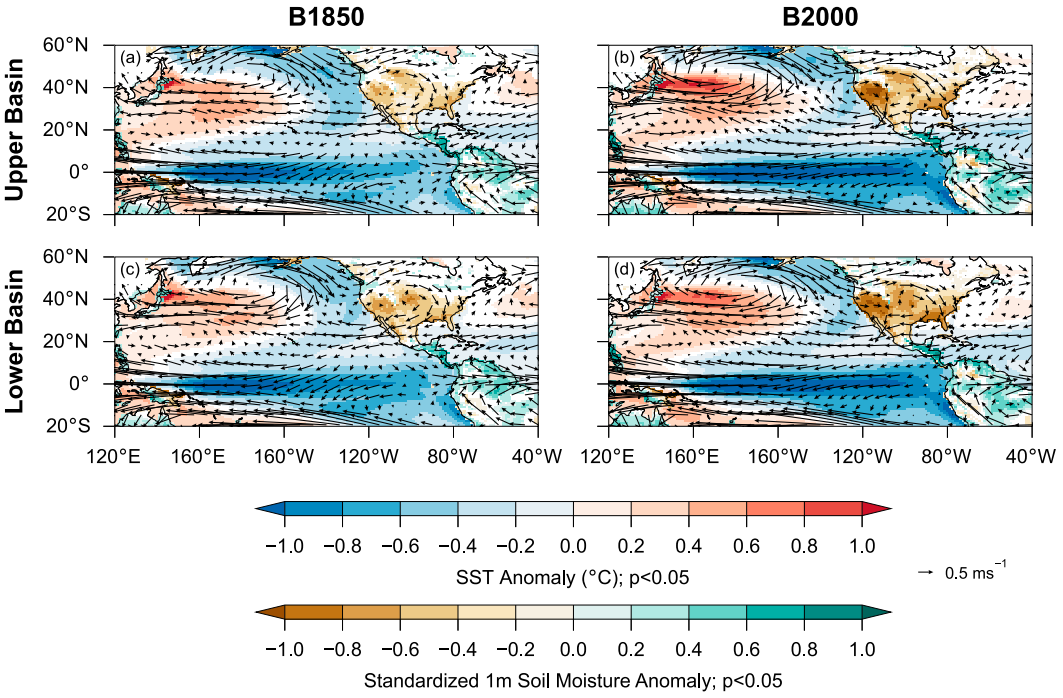

FIG. 9. When April–September basin average runoff is in the lower 20th percentile during La Niña events in 1940–2019, composite concurrent 700-hPa wind (vectors; m s^{-1}) and SST anomalies (blue–red shading; °C) and composite antecedent standardized 1-m soil moisture anomaly (brown–green shading; standard deviations) during the prior March for the (left) B1850 and (right) B2000 equilibrium simulations in the (top) UMRB and (bottom) LMRB. Shading for SSTs and 1-m soil moisture indicates anomalies that are statistically significant at $p < 0.05$.

which suggests the importance of land surface effects on the preconditioning of low runoff.

The equilibrium simulations also indicate that below-average snow water equivalent in March is related to low runoff in the Missouri River basin during the following April–September (Fig. 11). However, there are notable differences between each of the equilibrium simulations that principally reflect the effects of radiative forcing, which determines warmer and cooler climates of the B2000 and B1850 simulations (cf. Fig. 11, left column to Fig. 11, right column). The F1850 simulation reveals a close relationship between warm-season UMRB runoff and snow water equivalent in Montana—the headwaters for the Missouri River—just prior to the warm season, indicating the importance of this relationship in a climate without SST variability. This relationship is not particularly strong for the LMRB, however, because this subbasin lacks the considerable snowpack development during winter compared to the UMRB. The B1850 simulation, which shares the same atmospheric radiative forcing as the F1850 simulation, but with SST variability, displays a similar relationship between warm-season runoff and snow water equivalent prior to the warm season in the UMRB. This indicates that once snow water equivalent is in place in March that SST variability itself is not a principal intervening factor in determining its relationship with runoff in the following April–September.

A notable difference between the B2000 and B1850 simulations concerns the dissimilar relationships between low warm-season runoff and snow water equivalent just prior to the warm season (cf. Fig. 11, center column, and Fig. 11, right column). Unlike this relationship documented previously for the B1850 simulation, low runoff in the B2000 simulation in the UMRB is weakly related to antecedent snow water equivalent in the elevated areas of Montana that have historically served as the principal source for runoff in this subbasin. A reason for this is considerably less snow water equivalent is present in the B2000 climate compared to that of B1850 because high temperatures in the former compared to the latter reduce snow accumulation (Fig. S5). This suggests that causes of hydrological drought in a warmer climate are different from those in a cooler climate because the responsible physical mechanisms differ between them.

c. *Potential predictability*

Having identified several factors constraining Missouri River basin hydroclimate in April–September, we conclude with a quantification of potential predictability of drought in two consecutive warm seasons. Here, we use the relative risk ratio (see methods), which provides an indication for predictability based on the change in drought frequency given the presence of a predictor. For example, for an initial dry state of 1-m soil moisture in March, a nearly threefold increase in the drought risk exists for the first April–September and a nearly twofold increase in the risk of drought for the second April–September (Fig. 12). These results indicate that 2-yr warm-season droughts—or their

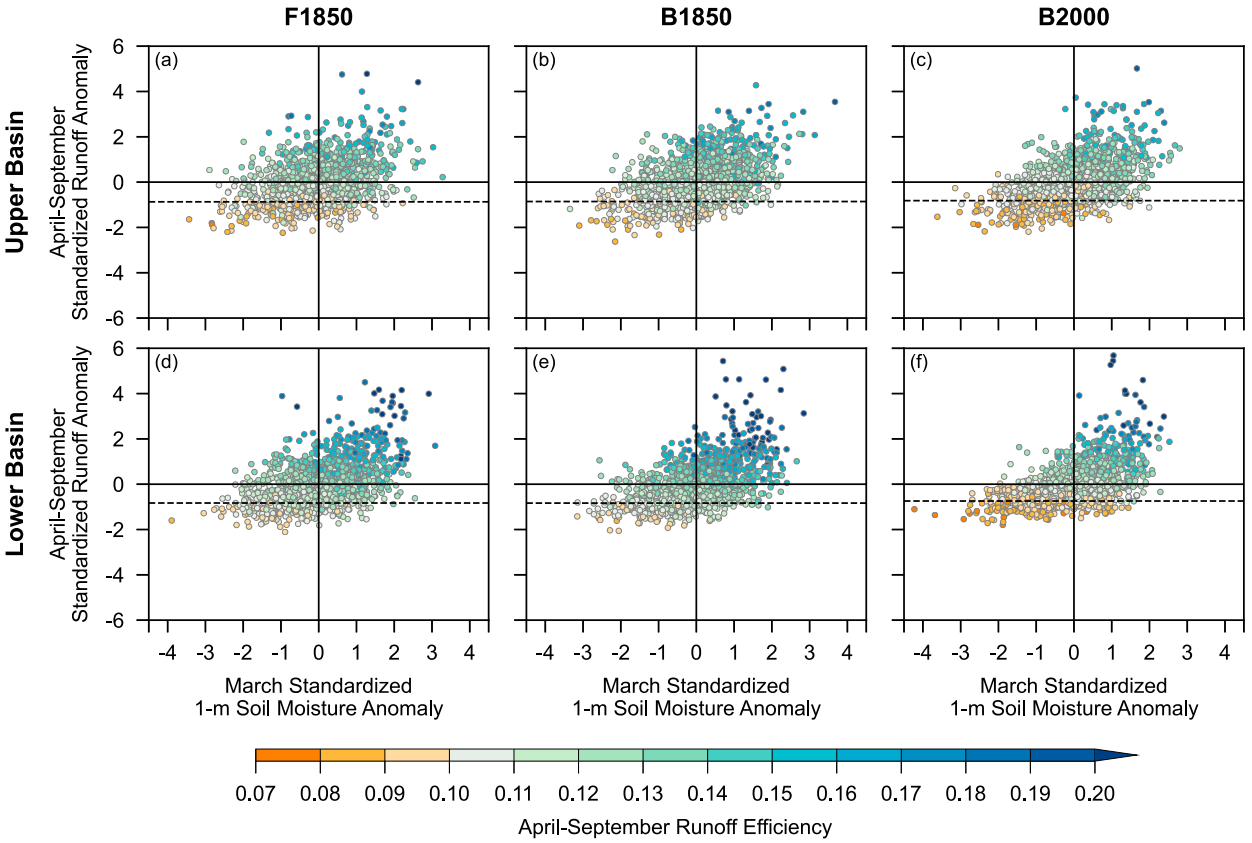

FIG. 10. Scatter diagram of April–September standardized runoff anomaly and standardized 1-m soil moisture anomaly from the prior March with shading indicating April–September runoff efficiency, defined as the fraction of runoff to precipitation for the (left) F1850, (center) B1850, and (right) B2000 equilibrium simulations in the (top) UMRB and (bottom) LMRB. Indicated by the dashed black line is the 20th percentile runoff in April–September.

absence—are potentially predictable based on the antecedent state of the land surface.

The initial state of snow water equivalent in March is related to statistically significant differences in the relative risk of UMRB and LMRB runoff in the warm season immediately following (Fig. 12), though having a somewhat smaller impact as measured by risk alone than initial soil moisture. This significant, though weaker constraint, is likely because the soil moisture signal is confined to a smaller fraction of the Missouri River basin overall, also accounting for its greater relevant to UMRB rather than LMRB warm-season runoff (Figs. 7 and 11). However, the state of snow water equivalent in March is not significantly related to differences in the relative risk of low runoff in a second consecutive April–September across all equilibrium simulations in the UMRB (Fig. 12). These results suggest that snow water equivalent is not a reliable potential predictor of low runoff in two consecutive warm seasons in the UMRB as we found for 1-m soil moisture. This is especially important in the UMRB, where we found that low warm-season runoff is more closely related to antecedent snow water equivalent compared to the LMRB. The B1850 simulation is the only equilibrium climate that indicates a significant increase in low runoff in consecutive warm seasons related to low snow water equivalent prior to the first. Potential reasons for this include a higher contribution to runoff by snow water equivalent in the B1850 simulation because of its cooler climate and greater snowpack in March compared to the B2000 simulation (Fig. S5).

The ENSO state in March is also related to statistically significant differences in the relative risk of low runoff during following April–September seasons, indicating that La Niña is a potential predictor of UMRB and LMRB drought (Fig. 12), though with an efficacy less than that exerted by initial soil moisture states. There are, however, notable relative risks of future warm-season drought related to La Niña between the B1850 and B2000 climates. The CESM1 simulations reveal La Niña to be a better predictor in the warmer than colder climate states, especially for the risks of drought in a second year. Potential reasons for this include a closer relationship between ENSO and Missouri River basin hydroclimate in the year 2000 climate compared to the year 1850 climate, a change in the teleconnection itself indicated in Fig. 8. Another possibility is that ENSO variability itself may change in the warmer climate, perhaps via stronger variance in tropical Pacific SSTs and a greater likelihood for La Niña events last for 2 years. These are intriguing issues that merit further investigation using a larger suite of coupled models.

Finally, we examine the potential predictability of low UMRB and LMRB runoff in consecutive April–September based on

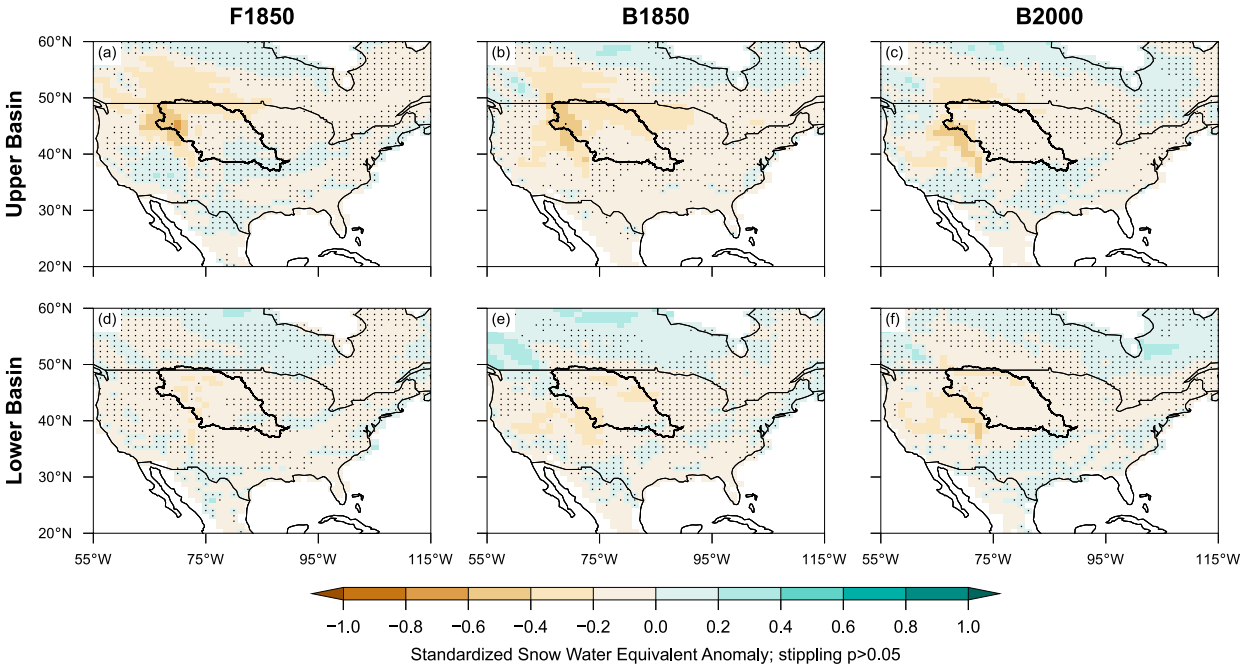

FIG. 11. Composite March standardized snow water equivalent anomaly when runoff during the following April–September is in the lower 20th percentile for the (left) F1850, (center) B1850, and (right) B2000 equilibrium simulations in the (top) UMRB and (bottom) LMRB. Stippling indicates the standardized departures that are not statistically significant at $p < 0.05$.

both 1-m soil moisture and ENSO states in the prior March, recognizing that anomalous behavior of both predictors could be operating at the same time. Figure 13 indicates that the combination of low 1-m soil moisture and La Niña in March greatly increases the relative risk of low runoff during the following April–September in the UMRB and LMRB beyond the individual effects of low soil moisture or La Niña (Fig. 12). The results are consistent between basins and simulations. Figure 13 also indicates that the combination of high soil moisture and La Niña in March decreases the risk of low UMRB and LMRB runoff during the April–September immediately following and does not significantly change the risk of low runoff in the subsequent April–September. This indicates that a wet antecedent land surface provides a buffer to avert low runoff in the presence of La Niña, which otherwise increases the likelihood of drought in the UMRB and LMRB (Fig. 12). Concerning El Niño, its presence generally leads to no difference in the risk of low warm-season runoff when combined with low 1-m soil moisture, which indicates its effects on averting drought in following warm seasons. Of the two subbasins and equilibrium simulations considered, this is not true for the LMRB and B1850 climate, perhaps a result of the relationship between LMRB hydroclimate in 1850 identified previously (Figs. 8 and 11).

5. Summary and conclusions

a. *What is the intrinsic persistence of Missouri River basin hydroclimate?*

Observed estimates and a transient coupled climate model ensemble based on CESM1 indicate persistent runoff and soil moisture anomalies in the UMRB and LMRB whose decorrelations depend on the seasonal cycles of precipitation and temperature. These results are similar to those found in prior studies that focused on different aspects of North American hydroclimate (e.g., Delworth and Manabe 1988; Koster and Suarez 2001; Rahman et al. 2015; Kumar et al. 2019). We principally focused on the persistent anomalies from March so we could examine how land surface memory preconditioned hydroclimate in future April–September wet seasons. Statistically significant serial runoff correlations from March indicate runoff persistence from the prior wet season into the next wet season, which is consistent with Badger et al. (2018). Likewise, statistically significant serial soil moisture correlations from March in the 30-cm and 1-m layers were also found, the largest of which were found in the dry season months leading up to March, with lower yet statistically significant correlations into the following wet season. The persistent land surface anomalies were not accompanied by persistent $P - E$ anomalies, as we found no statistically significant serial correlations in $P - E$. These persistent runoff and soil moisture anomalies motivated our diagnosis of multiyear low runoff predictability based on antecedent land surface soil moisture in the two subbasins that comprise the largest hydrologic catchment in North America (Seaber et al. 1987).

b. *How do land surface, atmosphere, and ocean features contribute droughts in warmer and cooler climates?*

We found that low April–September runoff in the UMRB and LMRB are related to inherent atmospheric variability, antecedent local soil moisture, snow water equivalent, and

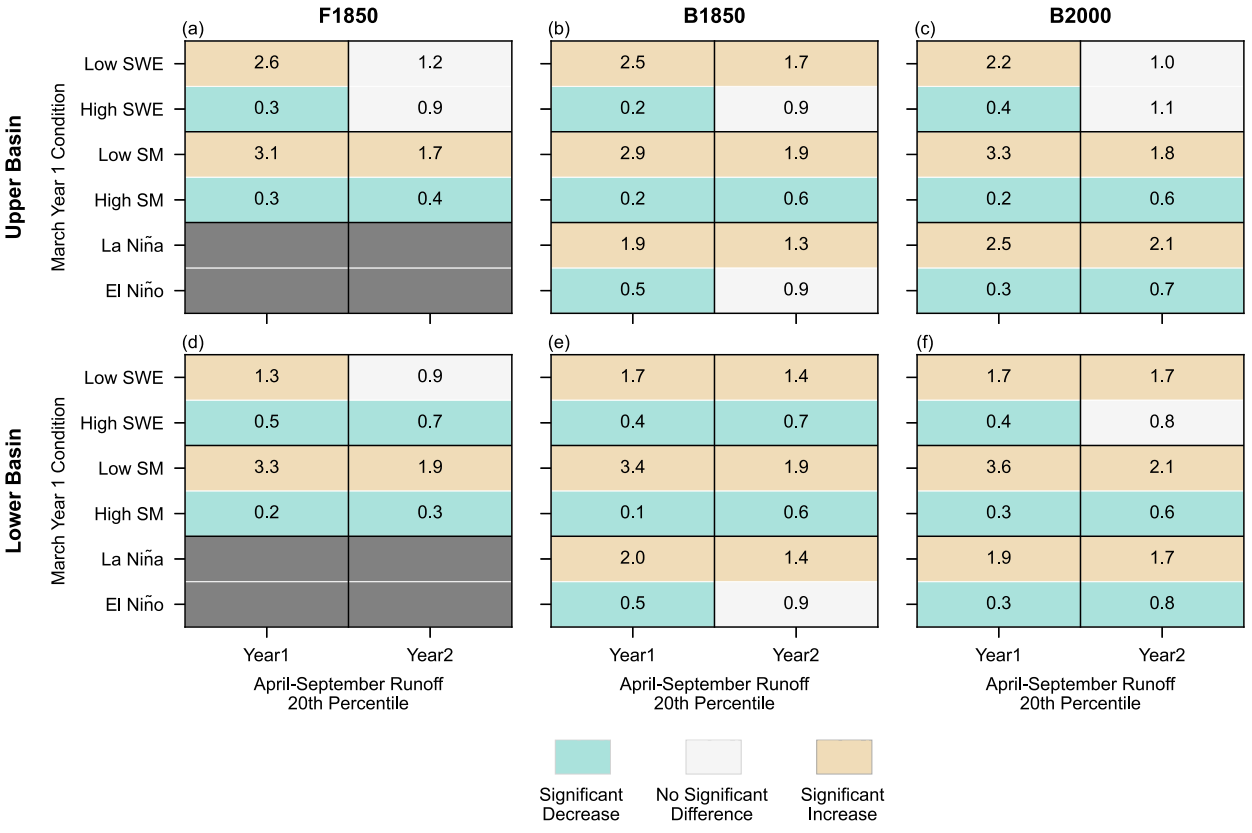

FIG. 12. Relative risk ratio of runoff falling in the lower 20th percentile in April–September of years 1 and 2 following low snow water equivalent, high snow water equivalent, low 1-m soil moisture, high 1-m soil moisture, La Niña, and El Niño in March prior to year 1 compared to when those conditions are not met based on (left) B1850, and (right) B2000 equilibrium simulations in the (top) UMRB and (bottom) LMRB. ENSO conditions are shaded in the F1850 simulation because there is no SST variability from the seasonal cycle.

remote tropical Pacific SST states associated with ENSO. Moreover, the relationship between low runoff, snow water equivalent, and ENSO is different in warmer and cooler climates, which indicates that anthropogenic effects alter the relationship between these physical features and warm-season drought, and, thus, also may alter their predictability. A key difference between prior studies concerning central United States drought under anthropogenic effects (e.g., Wehner et al. 2011; Cook et al. 2015) and our study is that we do not include secular changes related to atmospheric forcing based on our analysis of equilibrium simulations compared to their own climate. This perspective allows us to isolate the variability of drought in warmer and cooler climates (see also Cheng et al. 2019), which is important for assessing and responding to drought in a warmer world (Parker et al. 2023).

Inherent atmospheric variability and La Niña are related to atmospheric circulations that result in low UMRB and LMRB runoff during the warm season. Inherent atmospheric behaviors are indicated in the F1850 simulation (no SST variability from a prescribed annual cycle) by a wave train of alternating high and low pressure areas spanning the Pacific–North American sector with precipitation-suppressing high pressure over the central United States. La Niña is indicated by a wave train of high and low pressure areas emanating from the tropics associated with below-average SSTs in the tropical central Pacific Ocean that are associated with precipitation-suppressing high pressure over the central United States.

The relationship between La Niña and Missouri River basin drought in April–September is stronger in a warmer climate compared to a cooler climate, as indicated by larger SST and circulation anomalies in the former climate (B2000 simulation) compared to the latter (B1850 simulation). These results suggest that La Niña plays a larger role in driving UMRB and LMRB drought during the warm season and offering potential predictability under anthropogenic influences. Many climate models indicate that ENSO variability increases under anthropogenic influences (e.g., Cai et al. 2021), the effect of which would alter hydroclimates sensitive to La Niña like the central United States (e.g., Singh et al. 2022). CESM1, the model used in our study, indicates an increase in ENSO variability under increased radiative forcing (Newman et al. 2018; Berner et al. 2020; Maher et al. 2023).

Soil moisture and snow water equivalent anomalies are closely related to low April–September runoff in the UMRB and LMRB. The relationships between soil moisture within

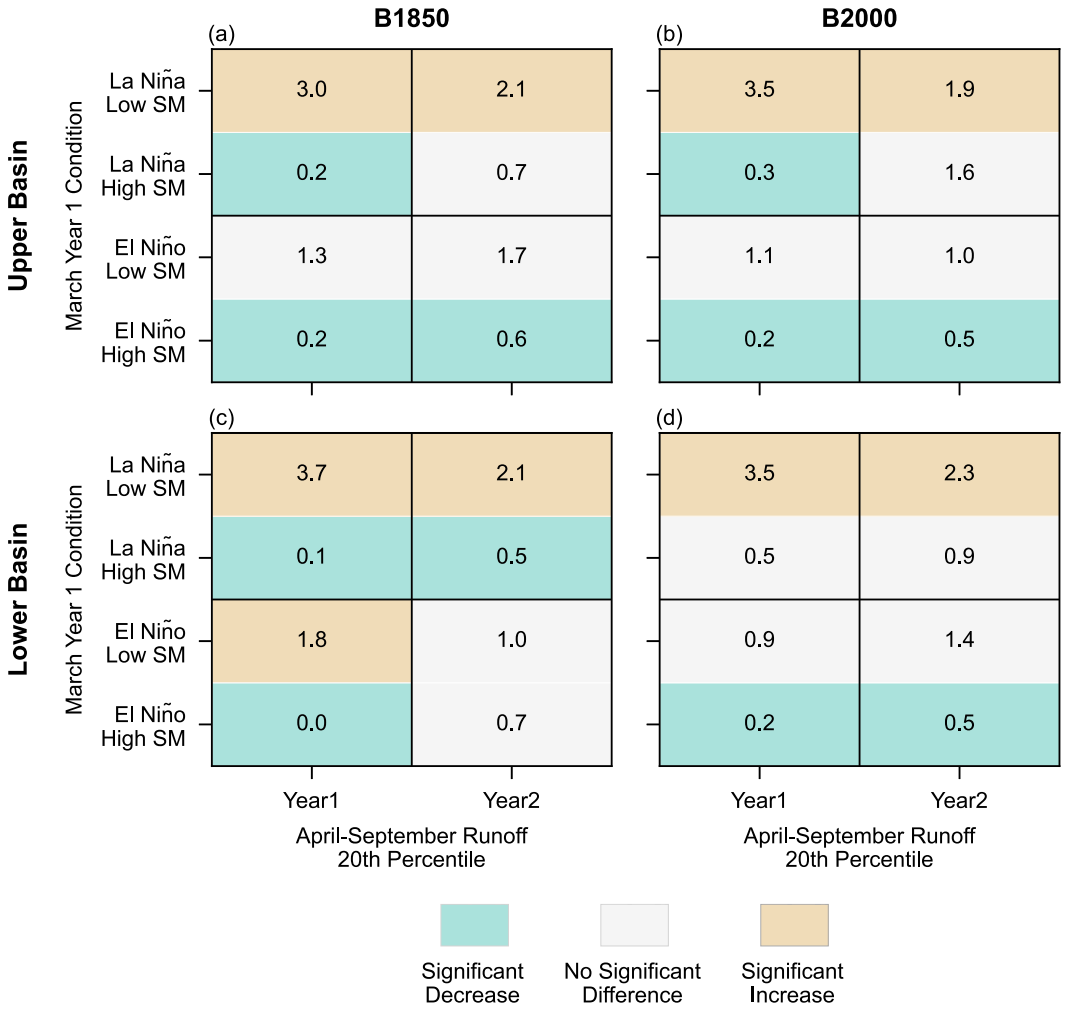

FIG. 13. Relative risk ratio of runoff falling in the lower 20th percentile in April–September of years 1 and 2 following combined low soil moisture and La Niña, combined high soil moisture and La Niña, combined low soil moisture and El Niño, combined high soil moisture and El Niño in March prior to year 1 compared to when those conditions are not met based on (left) B1850 and (right) B2000 equilibrium simulations in the (top) UMRB and (bottom) LMRB. The F1850 simulation is not shown because there is no ENSO variability.

the Missouri River basin and low runoff are similar in warmer and cooler climates as well as those without ENSO variability. Low soil moisture decreases runoff efficiency, which leads to more precipitation being used to replenish moisture in the soils and less being converted to runoff. By contrast, the relationship between snow water equivalent and runoff differs between UMRB and LMRB and warmer and cooler climates. Snowmelt-driven runoff was shown to be important in the UMRB (e.g., Norton et al. 2014; Wise et al. 2018), and it follows that we found a closer relationship between drought and snow water equivalent in the UMRB. We also found a closer relationship between drought and snow water equivalent in a cooler climate (B1850) than a warmer climate (B2000) related to notable decreases in snow water equivalent from the former to the latter. These results suggest a decreased role of snowpack in driving runoff in a warmer world.

c. *Can snow water equivalent, soil moisture, and ENSO state potentially predict 2-yr warm-season droughts?*

Snow water equivalent, soil moisture, and ENSO state in March are the potential predictors of 2-yr warm-season droughts in the UMRB and LMRB as indicated by their relationships with statistically significant changes in the relative risk of low runoff in future April–September seasons. Consistent with our analysis of mechanisms related to warm-season drought in the Missouri River basin, potential predictability of low runoff based on each of these three features in March differs between warmer and cooler climates, which suggests that anthropogenic effects influence drought predictability.

Soil moisture and snow water equivalent in March were found to be potential predictors of runoff in the following April–September, with the former related to larger relative risks of drought at longer lead times. Concerning 1-m soil

moisture, we found that the predictive information gained from soil moisture is consistent in warmer and cooler climates as well as climates without ENSO variability. Low 1-m soil moisture is related to statistically significant increases in the relative risk of low runoff in the two following April–September, while high 1-m soil moisture is related to statistically significant decreases in the relative risk of low runoff in the two following April–September. By contrast, the predictive power of snow water equivalent on runoff differs between the UMRB and LMRB and warmer and cooler climates. In the UMRB, low snow water equivalent in March is related to statistically significant increases in the risk of low runoff in the following April–September. The B1850 simulation is the only equilibrium climate that indicates a significant increase in the relative risk low UMRB runoff in two consecutive warm seasons related to low snow water equivalent prior to the first. Potential reasons include the importance of snowmelt-driven runoff in the UMRB (e.g., Norton et al. 2014; Wise et al. 2018) and notable reductions in snow water equivalent in the UMRB from cooler to warmer climates, the latter of which suggests a decrease in the prevalence of snowmelt-driven runoff in a warmer world.

Statistically significant changes in the risk of low runoff in April–September seasons were also found to follow ENSO events in March. Relative risks related to ENSO are not as large as the relative risks related to 1-m soil moisture, differ between warmer and cooler climates, and differ between La Niña and El Niño events. The larger relative risk of warm-season drought related to ENSO in the B2000 simulation compared to the B1850 simulation may be due to increased ENSO variability in the former compared to the latter in the CESM1 model under increased radiative forcing (Newman et al. 2018; Berner et al. 2020; Maher et al. 2023). Differences in statistically significant relative risks of drought related to La Niña and El Niño events suggest asymmetry in the hydroclimatic response to ENSO, which could be related to the asymmetric relationship between precipitation and opposing ENSO phases suggested by Wang et al. (2007).

The combination of high soil moisture and La Niña in March is related to statistically significant decreases in the risk of low runoff in the following April–September, which indicates that a wet land surface provides a buffer to avert low runoff in the presence of La Niña. Moreover, these results also suggest the primacy of the land surface state regarding future runoff compared to the state of ENSO. Our analysis also revealed that a dry land surface state combined with La Niña in March increased the likelihood of low runoff in two consecutive April–September compared to if just one of these conditions were operating.

A feature of La Niña events relevant to Missouri River basin drought in consecutive April–September concerns the propensity of such events to last multiple years (e.g., Okumura and Deser 2010; Okumura et al. 2011; Hu et al. 2014; Wu et al. 2019). While we did not specifically address this feature, the effects of multiyear La Niña events suggest prolonged dryness in the North American Great Plains that includes the Missouri River basin (e.g., Anderson et al. 2017; Jong et al. 2020), as was observed on occasion in the 1800s, the Dust Bowl (e.g., Schubert et al. 2004), and in the 1950s (Cole et al. 2002), for example. Multiyear La Niña events are potentially predictable at 6–25-month lead times based on CESM1, the model architecture we used in our study (DiNezio et al. 2017; Wu et al. 2021). These results also suggest that 2-yr droughts in the Missouri River basin may also be potentially predictable based on the predictability of La Niña itself, which could be a reason for statistically significant increases in the chances of low runoff in consecutive April–September in the LMRB based on La Niña in the first year. Moreover, future projections of ENSO events under increased greenhouse gas forcing, similar to our comparison of B2000 and B1850 simulations, indicate an increased likelihood of multiyear La Niña events (Geng et al. 2023). This increase in multiyear La Niña events due to anthropogenic forcing suggests an increase in the potential predictability of 2-yr droughts in the Missouri River basin.

Acknowledgments. The authors gratefully acknowledge two anonymous reviewers and Jon Eischeid for their helpful comments on an earlier version of this article, Ryan Larsen of the U.S. Army Corps of Engineers for providing naturalized Missouri River flow, and the support from the NOAA/Climate Program Office Modeling, Analysis, Predictions, and Projections Program, the National Integrated Drought Information System, and the NOAA Physical Sciences Laboratory.

Data availability statement. Observed estimates and climate model simulations are available from the sources listed in Tables 1 and 2, respectively. Naturalized Missouri River flow is available from the U.S. Army Corps of Engineers.

REFERENCES

Alexander, M. A., I. Bladé, M. Newman, J. R. Lanzante, N.-C. Lau, and J. D. Scott, 2002: The atmospheric bridge: The influence of ENSO teleconnections on air–sea interaction over the global oceans. *J. Climate*, **15**, 2205–2231, https://doi.org/10.1175/1520-0442(2002)015<2205:TABTIO>2.0.CO;2.

Anderson, W., R. Seager, W. Baethgen, and M. Cane, 2017: Life cycles of agriculturally relevant ENSO teleconnections in North and South America. *Int. J. Climatol.*, **37**, 3297–3318, https://doi.org/10.1002/joc.4916.

Badger, A. M., B. Livneh, M. P. Hoerling, and J. K. Eischeid, 2018: Understanding the 2011 Upper Missouri River Basin floods in the context of a changing climate. *J. Hydrol.*, **19**, 110–123, https://doi.org/10.1016/j.ejrh.2018.08.004.

Berner, J., H. M. Christensen, and P. D. Sardeshmukh, 2020: Does ENSO regularity increase in a warming climate? *J. Climate*, **33**, 1247–1259, https://doi.org/10.1175/JCLI-D-19-0545.1.

Burgdorf, A.-M., S. Brönnimann, and J. Franke, 2019: Two types of North American droughts related to different atmospheric circulation patterns. *Climate Past*, **15**, 2053–2065, https://doi.org/10.5194/cp-15-2053-2019.

Cai, W., and Coauthors, 2021: Changing El Niño–Southern Oscillation in a warming climate. *Nat. Rev. Earth Environ.*, **2**, 628–644, https://doi.org/10.1038/s43017-021-00199-z.

Cheng, L., M. Hoerling, Z. Liu, and J. Eischeid, 2019: Physical understanding of human-induced changes in U.S. hot droughts using equilibrium climate simulations. *J. Climate*, **32**, 4431–4443, https://doi.org/10.1175/JCLI-D-18-0611.1.

Christian, J. I., and Coauthors, 2024: Flash drought: A state of the science review. *WIREs Water*, **11**, e1714, https://doi.org/10.1002/wat2.1714.

Cole, J. E., J. T. Overpeck, and E. R. Cook, 2002: Multiyear La Niña events and persistent drought in the contiguous United States. *Geophys. Res. Lett.*, **29**, 1647, https://doi.org/10.1029/2001GL013561.

Conant, R. T., and Coauthors, 2018: Northern Great Plains. *Impacts, Risks, and Adaptation in the United States: Fourth National Climate Assessment, Volume II*, D. R. Reidmiller et al., Eds., U.S. Global Change Research Program, 941–986.

Cook, B. I., R. Seager, and R. L. Miller, 2011: Atmospheric circulation anomalies during two persistent North American droughts: 1932–1939 and 1948–1957. *Climate Dyn.*, **36**, 2339–2355, https://doi.org/10.1007/s00382-010-0807-1.

——, T. R. Ault, and J. E. Smerdon, 2015: Unprecedented 21st century drought risk in the American Southwest and Central Plains. *Sci. Adv.*, **1**, e1400082, https://doi.org/10.1126/sciadv.1400082.

Delworth, T. L., and S. Manabe, 1988: The influence of potential evaporation on the variabilities of simulated soil wetness and climate. *J. Climate*, **1**, 523–547, https://doi.org/10.1175/1520-0442(1988)001<0523:TIOPEO>2.0.CO;2.

DiNezio, P. N., C. Deser, Y. Okumura, and A. Karspeck, 2017: Predictability of 2-year La Niña events in a coupled general circulation model. *Climate Dyn.*, **49**, 4237–4261, https://doi.org/10.1007/s00382-017-3575-3.

Ding, Q., and B. Wang, 2005: Circumglobal teleconnection in the Northern Hemisphere summer. *J. Climate*, **18**, 3483–3505, https://doi.org/10.1175/JCLI3473.1.

Efron, B., 1979: Bootstrap methods: Another look at the jackknife. *Ann. Stat.*, **7**, 1–26, https://doi.org/10.1214/aos/1176344552.

Esit, M., S. Kumar, A. Pandey, D. M. Lawrence, I. Rangwala, and S. Yeager, 2021: Seasonal to multi-year soil moisture drought forecasting. *npj Climate Atmos. Sci.*, **4**, 16, https://doi.org/10.1038/s41612-021-00172-z.

Frederick, S. E., and C. A. Woodhouse, 2020: A multicentury perspective on the relative influence of seasonal precipitation on streamflow in the Missouri River Headwaters. *Water Resour. Res.*, **56**, e2019WR025756, https://doi.org/10.1029/2019WR025756.

Geng, T., F. Jia, W. Cai, L. Wu, B. Gan, Z. Jing, S. Li, and M. J. McPhaden, 2023: Increased occurrences of consecutive La Niña events under global warming. *Nature*, **619**, 774–781, https://doi.org/10.1038/s41586-023-06236-9.

Heim, R. R., Jr., 2017: A comparison of the early twenty-first century drought in the United States to the 1930s and 1950s drought episodes. *Bull. Amer. Meteor. Soc.*, **98**, 2579–2592, https://doi.org/10.1175/BAMS-D-16-0080.1.

Hersbach, H., and Coauthors, 2020: The ERA5 global reanalysis. *Quart. J. Roy. Meteor. Soc.*, **146**, 1999–2049, https://doi.org/10.1002/qj.3803.

Ho, M., U. Lall, and E. R. Cook, 2016: Can a paleodrought record be used to reconstruct streamflow? A case study for the Missouri River Basin. *Water Resour. Res.*, **52**, 5195–5212, https://doi.org/10.1002/2015WR018444.

Hoell, A., and Coauthors, 2020: Lessons learned from the 2017 flash drought across the U.S. Northern Great Plains and Canadian Prairies. *Bull. Amer. Meteor. Soc.*, **101**, E2171–E2185, https://doi.org/10.1175/BAMS-D-19-0272.1.

——, T. W. Ford, M. Woloszyn, J. A. Otkin, and J. Eischeid, 2021: Characteristics and predictability of midwestern United States drought. *J. Hydrometeor.*, **22**, 3087–3105, https://doi.org/10.1175/JHM-D-21-0052.1.

——, M. Hoerling, X.-W. Quan, and R. Robinson, 2023: Recent high Missouri River basin runoff was unlikely caused by climate change. *J. Appl. Meteor. Climatol.*, **62**, 657–675, https://doi.org/10.1175/JAMC-D-22-0158.1.

Hoerling, M., X.-W. Quan, and J. Eischeid, 2009: Distinct causes for two principal U.S. droughts of the 20th century. *Geophys. Res. Lett.*, **36**, L19708, https://doi.org/10.1029/2009GL039860.

Hornbeck, R., 2012: The enduring impact of the American Dust bowl: Short- and long-run adjustments to environmental catastrophe. *Amer. Econ. Rev.*, **102**, 1477–1507, https://doi.org/10.1257/aer.102.4.1477.

Hu, Q., S. Feng, and R. J. Oglesby, 2011: Variations in North American summer precipitation driven by the Atlantic multidecadal oscillation. *J. Climate*, **24**, 5555–5570, https://doi.org/10.1175/2011JCLI4060.1.

Hu, Z.-Z., A. Kumar, Y. Xue, and B. Jha, 2014: Why were some La Niñas followed by another La Niña? *Climate Dyn.*, **42**, 1029–1042, https://doi.org/10.1007/s00382-013-1917-3.

Huang, B., and Coauthors, 2017: Extended Reconstructed Sea Surface Temperature, version 5 (ERSSTv5): Upgrades, validations, and intercomparisons. *J. Climate*, **30**, 8179–8205, https://doi.org/10.1175/JCLI-D-16-0836.1.

Hurt, D. R., 1981: *The Dust Bowl: An Agricultural and Social History*. Nelson Hall, 214 pp.

Jong, B.-T., M. Ting, R. Seager, and W. B. Anderson, 2020: ENSO teleconnections and impacts on U.S. summertime temperature during a multiyear La Niña life cycle. *J. Climate*, **33**, 6009–6024, https://doi.org/10.1175/JCLI-D-19-0701.1.

Kay, J. E., and Coauthors, 2015: The Community Earth System Model (CESM) large ensemble project: A community resource for studying climate change in the presence of internal climate variability. *Bull. Amer. Meteor. Soc.*, **96**, 1333–1349, https://doi.org/10.1175/BAMS-D-13-00255.1.

Koster, R. D., and M. J. Suarez, 2001: Soil moisture memory in climate models. *J. Hydrometeor.*, **2**, 558–570, https://doi.org/10.1175/1525-7541(2001)002<0558:SMMICM>2.0.CO;2.

Kumar, S., M. Newman, Y. Wang, and B. Livneh, 2019: Potential reemergence of seasonal soil moisture anomalies in North America. *J. Climate*, **32**, 2707–2734, https://doi.org/10.1175/JCLI-D-18-0540.1.

——, ——, D. M. Lawrence, M.-H. Lo, S. Akula, C.-W. Lan, B. Livneh, and D. Lombardozzi, 2020: The GLACE-Hydrology experiment: Effects of land–atmosphere coupling on soil moisture variability and predictability. *J. Climate*, **33**, 6511–6529, https://doi.org/10.1175/JCLI-D-19-0598.1.

Livneh, B., M. Hoerling, A. Badger, and J. Eischeid, 2016: Causes for hydrologic extremes in the upper Missouri River basin. NOAA Climate Assessment Rep., 39 pp.

Maher, N., and Coauthors, 2023: The future of the El Niño–Southern Oscillation: Using large ensembles to illuminate time-varying responses and inter-model differences. *Earth Syst. Dyn.*, **14**, 413–431, https://doi.org/10.5194/esd-14-413-2023.

Mantua, N. J., S. R. Hare, Y. Zhang, J. M. Wallace, and R. C. Francis, 1997: A Pacific interdecadal climate oscillation with impacts on salmon production. *Bull. Amer. Meteor. Soc.*, **78**, 1069–1080, https://doi.org/10.1175/1520-0477(1997)078<1069:APICOW>2.0.CO;2.

Martin, J. T., and G. T. Pederson, 2022: Streamflow reconstructions from tree rings and variability in drought and surface water supply for the Milk and St. Mary River basins. *Quat.*

Sci. Rev., **288**, 107574, https://doi.org/10.1016/j.quascirev.2022.107574.

——, and Coauthors, 2020: Increased drought severity tracks warming in the United States' largest river basin. *Proc. Natl. Acad. Sci. USA*, **117**, 11 328–11 336, https://doi.org/10.1073/pnas.1916208117.

McCabe, G. J., M. A. Palecki, and J. L. Betancourt, 2004: Pacific and Atlantic Ocean influences on multidecadal drought frequency in the United States. *Proc. Natl. Acad. Sci. USA*, **101**, 4136–4141, https://doi.org/10.1073/pnas.0306738101.

——, and Coauthors, 2023: A hydrologic perspective of major U.S. droughts. *Int. J. Climatol.*, **43**, 1234–1250, https://doi.org/10.1002/joc.7904.

Mehta, V. M., N. J. Rosenberg, and K. Mendoza, 2011: Simulated impacts of three decadal climate variability phenomena on water yields in the Missouri River Basin. *J. Amer. Water Resour. Assoc.*, **47**, 126–135, https://doi.org/10.1111/j.1752-1688.2010.00496.x.

——, ——, and ——, 2012: Simulated impacts of three decadal climate variability phenomena on dryland corn and wheat yields in the Missouri River basin. *Agric. For. Meteor.*, **152**, 109–124, https://doi.org/10.1016/j.agrformet.2011.09.011.

Mo, K. C., L. N. Long, and J.-K. E. Schemm, 2012: Characteristics of drought and persistent wet spells over the United States in the atmosphere–land–ocean coupled model experiments. *Earth Interact.*, **16**, 1–26. https://doi.org/10.1175/2012EI000437.1.

National Integrated Drought Information System, 2020: Missouri River basin Drought Early Warning System (DEWS) strategic action plan. NOAA, 30 pp.

Newman, M., and Coauthors, 2016: The Pacific decadal oscillation, revisited. *J. Climate*, **29**, 4399–4427, https://doi.org/10.1175/JCLI-D-15-0508.1.

——, A. T. Wittenberg, L. Cheng, G. P. Compo, and C. A. Smith, 2018: The extreme 2015/16 El Niño, in the context of historical climate variability and change. *Bull. Amer. Meteor. Soc.*, **99**, S16–S20, https://doi.org/10.1175/BAMS-D-17-0116.1.

Norton, P. A., M. T. Anderson, and J. F. Stamm, 2014: Trends in annual, seasonal, and monthly streamflow characteristics at streamgages in the Missouri River watershed, water years 1960–2011. USGS Scientific Investigations Rep. 2014-5053, 128 pp.

Okumura, Y. M., and C. Deser, 2010: Asymmetry in the duration of El Niño and La Niña. *J. Climate*, **23**, 5826–5843, https://doi.org/10.1175/2010JCLI3592.1.

——, M. Ohba, C. Deser, and H. Ueda, 2011: A proposed mechanism for the asymmetric duration of El Niño and La Niña. *J. Climate*, **24**, 3822–3829, https://doi.org/10.1175/2011JCLI3999.1.

Otkin, J. A., M. Svoboda, E. D. Hunt, T. W. Ford, M. C. Anderson, C. Hain, and J. B. Basara, 2018: Flash droughts: A review and assessment of the challenges imposed by rapid-onset droughts in the United States. *Bull. Amer. Meteor. Soc.*, **99**, 911–919, https://doi.org/10.1175/BAMS-D-17-0149.1.

——, and Coauthors, 2022: Getting ahead of flash drought: From early warning to early action. *Bull. Amer. Meteor. Soc.*, **103**, E2188–E2202, https://doi.org/10.1175/BAMS-D-21-0288.1.

Parker, B. A., J. Lisonbee, E. Ossowski, H. R. Prendeville, and D. Todey, 2023: Drought assessment in a changing climate: Priority actions and research needs. NOAA Tech. Memo. OAR CPO-002, 96 pp.

Pendergrass, A. G., and Coauthors, 2020: Flash droughts present a new challenge for subseasonal-to-seasonal prediction. *Nat. Climate Change*, **10**, 191–199, https://doi.org/10.1038/s41558-020-0709-0.

Qiao, L., Z. Pan, R. B. Herrmann, and Y. Hong, 2014: Hydrological variability and uncertainty of lower Missouri River Basin under changing climate. *J. Amer. Water Resour. Assoc.*, **50**, 246–260, https://doi.org/10.1111/jawr.12126.

Rahman, M. M., M. Lu, and K. H. Kyi, 2015: Variability of soil moisture memory for wet and dry basins. *J. Hydrol.*, **523**, 107–118, https://doi.org/10.1016/j.jhydrol.2015.01.033.

Schubert, S. D., M. J. Suarez, P. J. Pegion, R. D. Koster, and J. T. Bacmeister, 2004: On the cause of the 1930s Dust Bowl. *Science*, **303**, 1855–1859, https://doi.org/10.1126/science.1095048.

——, ——, ——, ——, and ——, 2008: Potential predictability of long-term drought and pluvial conditions in the U.S. Great Plains. *J. Climate*, **21**, 802–816, https://doi.org/10.1175/2007JCLI1741.1.

Seaber, P. R., F. P. Kapinos, and G. L. Knapp, 1987: Hydrologic unit maps. USGS Water-Supply Paper 2294, 66 pp.

Seager, R., and M. Hoerling, 2014: Atmosphere and ocean origins of North American droughts. *J. Climate*, **27**, 4581–4606, https://doi.org/10.1175/JCLI-D-13-00329.1.

Shin, C.-S., B. Huang, P. A. Dirmeyer, S. Halder, and A. Kumar, 2020: Sensitivity of U.S. drought prediction skill to land initial states. *J. Hydrometeor.*, **21**, 2793–2811, https://doi.org/10.1175/JHM-D-20-0025.1.

Singh, J., M. Ashfaq, C. B. Skinner, W. B. Anderson, V. Mishra, and D. Singh, 2022: Enhanced risk of concurrent regional droughts with increased ENSO variability and warming. *Nat. Climate Change*, **12**, 163–170, https://doi.org/10.1038/s41558-021-01276-3.

Steinbeck, J., 1939: *The Grapes of Wrath*. Penguin Publishing Group, 528 pp.

Svoboda, M., and Coauthors, 2002: The Drought Monitor. *Bull. Amer. Meteor. Soc.*, **83**, 1181–1190, https://doi.org/10.1175/1520-0477-83.8.1181.

Taylor, K. E., R. J. Stouffer, and G. A. Meehl, 2012: An overview of CMIP5 and the experiment design. *Bull. Amer. Meteor. Soc.*, **93**, 485–498, https://doi.org/10.1175/BAMS-D-11-00094.1.

Teng, H., G. Branstator, A. B. Tawfik, and P. Callaghan, 2019: Circumglobal response to prescribed soil moisture over North America. *J. Climate*, **32**, 4525–4545, https://doi.org/10.1175/JCLI-D-18-0823.1.

Ting, M., and H. Wang, 1997: Summertime U.S. precipitation variability and its relation to Pacific sea surface temperature. *J. Climate*, **10**, 1853–1873, https://doi.org/10.1175/1520-0442(1997)010<1853:SUSPVA>2.0.CO;2.

U.S. Army Corps of Engineers, 2018: Missouri River mainstem reservoir system: Master water control manual, Missouri River Basin. Northwestern Division USACE, 284 pp.

Vose, R. S., and Coauthors, 2014: Improved historical temperature and precipitation time series for U.S. climate divisions. *J. Appl. Meteor. Climatol.*, **53**, 1232–1251, https://doi.org/10.1175/JAMC-D-13-0248.1.

Wang, Z., C.-P. Chang, and B. Wang, 2007: Impacts of El Niño and La Niña on the U.S. climate during northern summer. *J. Climate*, **20**, 2165–2177, https://doi.org/10.1175/JCLI4118.1.

Wehner, M., D. R. Easterling, J. H. Lawrimore, R. R. Heim Jr., R. S. Vose, and B. D. Santer, 2011: Projections of future drought in the continental United States and Mexico. *J. Hydrometeor.*, **12**, 1359–1377, https://doi.org/10.1175/2011JHM1351.1.

Wise, E. K., C. A. Woodhouse, G. J. McCabe, G. T. Pederson, and J.-M. St-Jacques, 2018: Hydroclimatology of the Missouri River basin. *J. Hydrometeor.*, **19**, 161–182, https://doi.org/10.1175/JHM-D-17-0155.1.

Woodhouse, C. A., and E. K. Wise, 2020: The changing relationship between the upper and lower Missouri River basins during drought. *Int. J. Climatol.*, **40**, 5011–5028, https://doi.org/10.1002/joc.6502.

Wu, R., and J. L. Kinter III, 2009: Analysis of the relationship of U.S. droughts with SST and soil moisture: Distinguishing the time scale of droughts. *J. Climate*, **22**, 4520–4538, https://doi.org/10.1175/2009JCLI2841.1.

Wu, X., Y. M. Okumura, and P. N. DiNezio, 2019: What controls the duration of El Niño and La Niña events? *J. Climate*, **32**, 5941–5965, https://doi.org/10.1175/JCLI-D-18-0681.1.

——, ——, C. Deser, and P. N. DiNezio, 2021: Two-year dynamical predictions of ENSO event duration during 1954–2015. *J. Climate*, **34**, 4069–4087, https://doi.org/10.1175/JCLI-D-20-0619.1.